MARMARA UNIVERSITY

INSTITUTE FOR GRADUATE STUDIES
IN PURE AND APPLIED SCIENCES

BALANCING OF 3-RPR PLANAR PARALLEL ROBOTS PASSING THROUGH SINGULAR CONFIGURATIONS

CEM SÜÜLKER

MASTER THESIS

Department of Mechanical Engineering

Thesis Supervisor

Assoc. Prof. Dr. Mustafa ÖZDEMİR

ISTANBUL, 2018

MARMARA UNIVERSITY

INSTITUTE FOR GRADUATE STUDIES
IN PURE AND APPLIED SCIENCES

BALANCING OF 3-RPR PLANAR PARALLEL ROBOTS PASSING THROUGH SINGULAR CONFIGURATIONS

CEM SÜÜLKER

(524616018)

MASTER THESIS

Department of Mechanical Engineering

Thesis Supervisor

Assoc. Prof. Dr. Mustafa ÖZDEMİR

ISTANBUL, 2018

MARMARA UNIVERSITY
INSTITUTE FOR GRADUATE STUDIES IN PURE AND APPLIED SCIENCES

Cem SÜÜLKER, a Master of Science student of Marmara University Institute for Graduate Studies in Pure and Applied Sciences, defended his thesis entitled "BALANCING OF 3-RPR PLANAR PARALLEL ROBOTS PASSING THROUGH SINGULAR CONFIGURATIONS", on September 18, 2018 and has been found to be satisfactory by the jury members.

Jury Members

Assoc. Prof. Dr. Mustafa ÖZDEMİR (Advisor)
Marmara University .....(SIGN) M. Özdemir

Prof. Dr. Bülent EKİCİ (Jury Member)
Marmara University .....(SIGN) .....

Assist.Prof. Dr. Hatice MERCAN (Jury Member)
Yıldız Technical University .....(SIGN) .....

APPROVAL

Marmara University Institute for Graduate Studies in Pure and Applied Sciences Executive Committee approves that Cem SÜÜLKER be granted the degree of Master of Science in Department of Mechanical Engineering on 08.10.2018. (Resolution no: 2018/25-02).

Director of the Institute
Prof. Dr. Bülent EKİCİ

ACKNOWLEDGMENT

I would like to thank to Assoc. Prof. Dr. Mustafa ÖZDEMİR for his precious advices and encouragement through this thesis. I also want to thank to my family for their support.

TABLE OF CONTENTS

ÖZET

TEKİL KONUMLARDAN GEÇEN 3-RPR DÜZLEMSEL PARALEL ROBOTLARIN DENGELENMESİ

Paralel robotlar, seri muadillerine kıyasla birtakım üstünlüklere sahiptir, ve bu nedenle sanayide yaygın bir şekilde kullanılırlar. Bu robotlara özgü Tip II tekillik problemi literatürde geniş ölçüde çalışılmıştır. Genel itibariyla gereken eyleyici kuvvetleri bu tekil konfigurasyonlar civarında sonsuza ıraksar, ve robotun kontrol edilebilirliği kaybolur. Tekilliklere karşı gürbüz dengeleme yöntemi Tip II tekilliklerden geçmek için geliştirilen en son metotlardan biridir. Literatürdeki hareket planlama yöntemleri istenen herhangi bir yörüngeyi takip etmede yardımcı olamaz, ancak tekilliklere karşı gürbüz dengeleme yöntemi ile bütün yörüngeler gerçeklenebilir. Bu tezde, tekilliklere karşı gürbüz dengeleme yöntemi, her bir bacağa birer tane sabitlenmek suretiyle, üç karşı ağırlık kullanarak 3-RPR düzlemsel paralel robotlara uygulanmıştır. Denge tasarım denklemi çıkarılmış ve karşı ağırlıkların uygun konumları analiz edilmiştir. Bu kapsamda iki teorem ve iki sonuç teoremi verilmiş ve ispatlanmıştır. Teorik olarak elde edilen sonuçlar sayısal örneklerle de doğrulanmıştır. Bu amaçla farklı dengeleme senaryoları incelenip biribiryle karşılaştırılmıştır. Dengeleme parametrelerinin robotun performansı üzerindeki etkisi, eyleyici kuvvetlerinin azaltılmasına dayanan bir performans indeksini baz alarak tartışılmıştır.

ABSTRACT

BALANCING OF 3-RPR PLANAR PARALLEL ROBOTS PASSING THROUGH SINGULAR CONFIGURATIONS

Parallel robots offer a number of superiorities over their serial counterparts, and for this reason they are widely used in industry. Type II singularity problem that is characteristic to these robots has been studied extensively in the literature. In general, the required actuator forces grow unboundedly around these singular configurations, and controllability of the robot is lost around them. The singularity robust balancing method is one of the recent methods that has been developed for crossing Type II singularities. Motion planning methods in the literature cannot help to track an arbitrarily desired trajectory; however, by using this recent method, every trajectory is realizable. In this thesis, the singularity robust balancing method is applied to 3-RPR planar parallel robots by using three counterweights, each being fixed to one separate leg. The balance design equation is obtained and suitable loci of counterweights are analyzed. Two theorems and two corollaries are given and proved within this context. The theoretical findings are also validated through numerical examples. Different balancing scenarios are considered and compared for this purpose. The effects of balancing parameters on the performance of the robot are discussed by considering a performance index that is based on decreasing the actuator efforts.

SYMBOLS

a_i : Distance between the base joints of the manipulator $(i = 1, 2x, 2y)$.

$\mathbf{A}$: Right-hand side coefficient matrix of the dynamics equations.

A_i : i'th base joint of the manipulator $(i = 1, \cdots, 3)$.

$\mathbf{A}^*$: Submatrix of $\mathbf{A}$ as constructed in Equation (3.30).

b_i : Dimensions associated with the moving platform $(i = 1, \cdots, 3)$.

B_i : Connection point of the i'th leg to the moving platform $(i = 1, \cdots, 3)$.

C_i : Coefficients to be evaluated at the singularity $(i = 1, \cdots, 5, x, x_1,$

$y, y_1, y_2, y_3, y_4, z, z_1)$.

c_i : $\cos(\theta_i)$

$c_{i'}$: $\cos(\theta_i + \alpha)$

$c_{i''}$: $\cos(\theta_i + \beta)$

c_{ij} : $\cos(\theta_i - \theta_j)$

$c_{ij'}$: $\cos(\theta_i - \theta_j - \alpha)$

$c_{ij''}$: $\cos(\theta_i - \theta_j - \beta)$

e : Euler's number.

$\mathbf{F}$: Vector of generalized actuator forces.

F_i : Force applied by the i'th linear actuator $(i = 1, \cdots, 3)$.

g : Gravitational acceleration.

g_i : Mass center distance of the i'th moving link $(i=1,\cdots,7)$.

G_i : Mass center of the i'th moving link $(i=1,\cdots,7)$.

G_{ci} : Mass center of the i'th counterweight $(i=1,\cdots,3)$.

$\mathbf{h}$: Right-hand side vector of velocity-level kinematic relations in Equation (2.20).

$\dot{\mathbf{h}}$: Time derivative of matrix $\mathbf{h}$.

i : $\sqrt{-1}$

I_i : Centroidal mass moment of inertia of the i'th moving link $(i=1,\cdots,7)$.

I_c : Centroidal mass moment of inertia of each of identical and identically located counterweights.

I_{ci} : Centroidal mass moment of inertia of the i'th counterweight $(i=1,\cdots,3)$.

$\mathbf{J}$: Jacobian matrix constructed as in Equation (2.21).

$\mathbf{J_c}$: Jacobian matrix of the constraint equations.

$\mathbf{J_t}$: Jacobian matrix of the task equations.

$\dot{\mathbf{J}}$: Time derivative of Jacobian matrix.

$\dot{J}_{ij}$: i'th row, j'th column element of matrix $\dot{\mathbf{J}}$ $(i=1,\cdots,7,\ j=1,\cdots,7)$.

K : Total kinetic energy of the robot.

L : Lagrangian function.

m_i : Mass of the i'th moving link $(i=1,\cdots,7)$.

m_c : Mass of each of identical and identically located counterweights.

m_{ci} : Mass of the i'th counterweight $(i=1,\cdots,3)$.

$\mathbf{M}$: Generalized inertia matrix.

M_{ij} : i'th row, j'th column element of matrix $\mathbf{M}$ $(i=1,\cdots,7,\ j=1,\cdots,7)$.

$\mathbf{N}$: Vector of the Coriolis, centrifugal and gravity forces in the dynamic equations of the robot.

N_i : i'th element of vector $\mathbf{N}$ $(i=1,\cdots,7)$.

P : End-point of the robot.

PI : Performance index given by Equation (5.1).

$\mathbf{q}$: Vector of generalized coordinates.

$\dot{\mathbf{q}}$: First time derivative of vector $\mathbf{q}$.

$\ddot{\mathbf{q}}$: Second time derivative of vector $\mathbf{q}$.

$\mathbf{r_{ci}}$: Position vector of the mass center of the i'th counterweight $(i=1,\cdots,3)$.

r_i : A_iG_{ci} $(i=1,\cdots,3)$

$\mathbf{r_{G_i}}$: Position vector of the mass center of the i'th moving link $(i=1,\cdots,7)$.

$\mathbf{R_i}$: i'th row of $\mathbf{A}^*$ matrix $(i=1,\cdots,4)$.

s_i : $\sin(\theta_i)$

$s_{i'}$: $\sin(\theta_i+\alpha)$

$s_{i''}$: $\sin(\theta_i+\beta)$

s_{ij} : $\sin(\theta_i-\theta_j)$

$s_{ij'}$: $\sin\left(\theta_i - \theta_j - \alpha\right)$

$s_{ij''}$: $\sin\left(\theta_i - \theta_j - \beta\right)$

$s(t)$: Time parametrizing function of the path.

t_f : End time of the task.

x : The coordinate as shown in Figure 2.1.

x_0 : Initial position of the end-point in the $x-$direction.

x_P : Position of the end-point in the $x-$direction.

x_s : x coordinate of the singular point in the numerical example.

x' : The coordinate as shown in Figure 3.2.

$x(t)$: Trajectory along $x-$axis.

$\mathbf{X}$: Vector of task variables.

$\dot{\mathbf{X}}$: Time derivative of vector $\mathbf{X}$.

$\mathbf{W}$: Left-hand side vector of the dynamic equations of the balanced robot.

$\mathbf{W}^*$: Subvector of $\mathbf{W}$ as constructed in Equation (3.33).

W_i^* : i'th element of vector $\mathbf{W}^*$ $(i = 1, \cdots, 4)$.

V : Total potential energy of the robot.

$\mathbf{V_{ci}}$: Velocity of the mass center of the i'th counterweight $(i = 1, \cdots, 3)$.

$\mathbf{V_{G_i}}$: Velocity of point G_i $(i = 1, \cdots, 7)$.

y : The coordinate as shown in Figure 2.1.

y_0 : Initial position of the end-point in the $y-$direction.

y_P : Position of the end-point in the $y-$direction.

y_s : y coordinate of the singular point in the numerical example.

y' : The coordinate as shown in Figure 3.2.

$y(t)$: Trajectory along $y-$axis.

z_i : Constant terms used while obtaining the trajectory in the numerical example.

α : Angle shown in Figure 2.1.

β : Angle shown in Figure 2.1.

γ : Angle shown in Figure 2.1.

δ : Angular position of each of identical and identically located counterweights.

δ_i : Angle shown in Figure 3.1 $(i=1,\cdots,3)$.

ϕ : Constant used in Equation (3.45).

ψ : Angle between the linear path and the $x-$axis in the numerical example (Figure 4.1).

$\boldsymbol{\lambda}$: Vector of Lagrange multipliers.

λ_i : i'th Lagrange multiplier $(i=1,\cdots,4)$.

$\boldsymbol{\mu}$: Combined vector of the actuator forces and Lagrange multipliers.

θ_i : Angular joint variables shown in Figure 2.1 $(i=1,\cdots,4)$.

$\dot{\theta}_i$: First time derivative of θ_i $(i=1,\cdots,4)$.

$\ddot{\theta}_i$: Second time derivative of θ_i $(i=1,\cdots,4)$.

ξ_i : A_iB_i $(i=1,\cdots,3)$

$\dot{\xi}_i$: First time derivative of ξ_i $(i=1,\cdots,3)$.

$\ddot{\xi}_i$: Second time derivative of ξ_i $(i=1,\cdots,3)$.

$\mathbf{\Delta}$: Vector that contains the terms due to the counterweights in the dynamic equations of balanced robot.

Δ_i : i'th element of $\mathbf{\Delta}$ vector $(i=1,\cdots,7)$.

ΔK : Additional kinetic energy stored by the counterweights.

ΔL : Additional terms appearing in the Lagrangian function due to the counterweights.

ΔV : Additional potential energy stored by the counterweights.

ρ : Radius of the circle described in Theorem 1.

τ_i : Generalized force associated with the generalized coordinate q_i $(i=1,\cdots,7)$.

$|\mathbf{A}|$: Determinant of matrix $\mathbf{A}$.

$|F_i|$: Absolute value of F_i $(i=1,\cdots,3)$.

LIST OF FIGURES

LIST OF TABLES

1. INTRODUCTION

Parallel robots are more and more preferred than serial ones because of their higher acceleration ability, precision, rigidity, and payload-carrying capability [1-4]. However, their main drawback is that there is singularity problem. There are three types of singularities for parallel robots. Type I singularities are often encountered at the workspace boundaries [5]; therefore, it can be said that they are not critical. Type II singularities are characteristically seen only in parallel manipulators due to their closed-loop architecture [5]. They occur within the workspace and highly decrease the controllability around them [6,7]. A Type III singularity happens when a Type I and a Type II singularity occurs simultaneously but this third kind of singularity can be eliminated by a proper kinematic design of the structure [8].

Thus researches on singularities of parallel manipulators have been mainly about overcoming the problems related to Type II singularities. There are several methods proposed to deal with them. One of these is the singularity free path planning [9]. This method is about avoiding singular configurations while planning the path of the motion. One drawback of this method is that usable workspace of the robot decreases. Another method to overcome the problem is the introduction of redundant actuators [10,11]. Since the use of redundant actuators increases the total cost of the system, there have been developed relatively less expensive methods. Sacrificing the control of a degree of freedom of the robot [12] is another method that is worth mentioning. However the use of this method decreases the controlled degrees of freedom of the manipulator while passing through the singular positions.

A more preferable recent solution for problems caused by Type II singularities is to pass through the singular points by satisfying certain conditions, namely, “the consistency conditions” [13,14]. These conditions were also further studied for their physical meaning [15,16]. Recently, Özdemir proved that consistency of the dynamic model at a Type II singular configuration is necessary but not sufficient to pass through that configuration [17]. The additional conditions were also derived by him [17].

Other than these, Özdemir studied on different methods that can be alternatively used for satisfying the consistency of the dynamic model. These are the singularity robust balancing method [18], which will be used in this thesis, and the singularity consistent payload placement technique [19,20]. Both of these techniques can be used to follow inconsistent trajectories. Singularity robust balancing method is to pass through an inconsistent trajectory by using balancing elements, like counterweights, elastic elements, and dampers. Singularity consistent payload placement method requires to place the payload on the end-effector platform so that the dynamic equations are consistent at the singularity.

Other than the aforementioned papers, some other recent studies on singularities of parallel manipulators are as follows: Karimi et al. [21] worked on avoiding singularities of 3-RPR parallel manipulator by using dimensional synthesis and self-reconfigurability. Li et al. [22] focused on elimination of type II singularities of 3T1R mechanism by using actuation redundancy. Liu et al. [23] concentrated on singularity-free path-planning of a 3-RRR robot by switching between working modes. Kaloorazi et al. [24] worked on singularity free workspace of 3-RPR and 6-UPS manipulators, and Liu et al. [25] on that of 4-RRR redundant manipulators. In a different context, Özdemir and İder [26] proposed a switching controller for passing through singular points.

Balancing which is also within the scope of this thesis has been mainly studied under two headings: static balancing and dynamic balancing. Other than these two types, singularity robust balancing method [18] can be considered as a third type of balancing method. Static balancing of parallel manipulators has been a considerable research field in the last decade [27,28]. The main purpose of static balancing is to overcome the effects of link weights and reducing the needed driving torques (or forces). Counterweight and elastic element methods are the two ways to statically balance a parallel manipulator. Counterweight method basically relies on the placement of counterweights such that the center of mass of the moving system is kept stationary along the gravity direction [29]. Elastic element method keeps the potential energy of the system constant by properly using springs [30]. These methods were studied for

different parallel manipulators in the literature [31-35]. Also, these two methods can be used together [36].

The main goal of dynamic balancing is to compensate shaking forces and shaking moments. Three widely used dynamic balancing methods are use of counter-mass and counter-rotation [37-40], use of four-bars [41,42] and counter mechanisms [43], and generation of optimal trajectories [44,45]. One drawback of counter-mass counter-rotation method is that it increases total mass and total inertia of the system [46-48]. Balancing a four-bar mechanism is easier than balancing a complex mechanism so dynamically balanced four-bar mechanisms can be used in order to balance complex systems. However, this method may further increase the overall complexity of the mechanism. It is worth to mention at this point that a dynamically balanced system is also statically balanced but not vice versa [49]. For more details about dynamic balancing, readers are referred to References [50] and [51].

Even though the singularity problem and balancing methods are still active research subjects, singularity robust balancing concept is a very recent technique proposed by Özdemir [18] in 2016. With this new concept, inconsistent trajectories can be passed through. This study aims to further study this recently proposed method of singularity robust balancing [18] by focusing on a planar parallel manipulator. The mostly used three degrees of freedom planar parallel mechanisms have 3-RPR [52-55], 3-RRR [56-59], or 3-PRR [60-63] structures. These manipulators are still under extensive research [64-68].

1.1. Aim and Scope of the Thesis

The aim of this thesis is to analyze the singularity robust balancing of 3-RPR planar parallel robots. In order to achieve this goal, first its balance design equation is derived. Then, by studying it analytically, two theorems and two corollaries are proposed and proved. Finally, different balancing alternatives are discussed by considering a performance index.

1.2. Outline of the Thesis

Chapter 2 presents kinematic and dynamic analyses of a 3-RPR mechanism. Dynamic equations are obtained by using the Lagrangian method, and type II singular configurations are determined.

Chapter 3 applies the singularity robust balancing method to the mechanism. Again Lagrangian method is used, and the singularity robust balance design equation is derived. Then by using this equation, possible counterweight loci are obtained. Two theorems and two corollaries are stated and proved in this regard.

In chapter 4, a numerical example is considered. A task which requires crossing a Type II singularity is prescribed. Without balancing, the mechanism cannot track the prescribed trajectory since the necessary actuator inputs are unbounded in the vicinity of the singularity. But, after balancing is applied to the mechanism, it can follow the trajectory since the required actuator forces remain bounded in the neighborhood of the singularity.

Then, in chapter 5, in order to get better insights, different balancing alternatives are compared by considering a performance index. Finally, chapter 6 summarizes the findings and gives conclusions.

2. KINEMATIC AND DYNAMIC ANALYSIS OF THE ROBOT

In this work, a 3-RPR mechanism will be considered. Figure 2.1 shows a 3-RPR planar parallel robot. The manipulator is driven by three linear actuators. Thus, the active joint variables are $A_1B_1 = \xi_1$, $A_2B_2 = \xi_2$, $A_3B_3 = \xi_3$. The actuator forces associated with ξ_1, ξ_2 and ξ_3 are shown by F_1, F_2 and F_3, respectively.

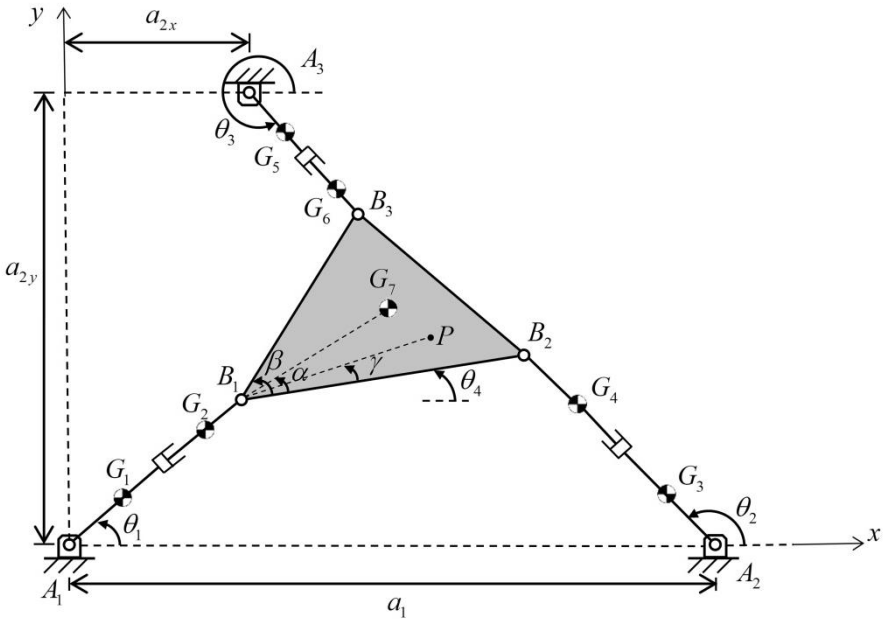

Figure 2.1 A 3-RPR manipulator

The mass center of link k is located at point G_k, and it has a mass m_k and a centroidal moment of inertia I_k $(k = 1, \cdots, 7)$. Table 2.1 gives the centroid locations of the moving links of the robot. The dimensions associated with the moving platform are $B_1B_2 = b_1$, $B_1B_3 = b_2$, $B_1P = b_3$.

Table 2.1 Mass center locations of the moving links

Mass center distance	Symbol
A_1G_1	g_1
B_1G_2	g_2
A_2G_3	g_3
B_2G_4	g_4
A_3G_5	g_5
B_3G_6	g_6
B_1G_7	g_7

Point A_1 is the origin of the fixed coordinate system xy.The gravity acceleration g is taken to be along the negative $y-$direction. In the formulations the cosine and sine functions are shown by c and s, respectively, whereas their argument angles are denoted as subscripts. These subscripts are as follows: i denotes the angle θ_i, i' the angle $\theta_i+\alpha$, i'' the angle $\theta_i+\beta$, ij the angle $\theta_i-\theta_j$, ij' the angle $\theta_i-\theta_j-\alpha$, ij'' the angle $\theta_i-\theta_j-\beta$ where $i,j=1,2,3,4$ (see also the Symbols section of the thesis).

2.1. Kinematic Analysis

There are two closed loops of this system. Loop closure equations can be written by disconnecting and reconnecting joints B_2 and B_3. First loop is chosen as $A_1-B_1-B_2-A_2-A_1$ and the corresponding equation is written as follows:

$$\overrightarrow{A_1B_1}+\overrightarrow{B_1B_2}=\overrightarrow{A_1A_2}+\overrightarrow{A_2B_2} \tag{2.1}$$

$$\xi_1 e^{i\theta_1}+b_1 e^{i\theta_4}=a_1+\xi_2 e^{i\theta_2} \tag{2.2}$$

It is possible to decompose Equation (2.2) into its real and imaginary components. Imaginary part is given as y coordinate and real part is given as x coordinate.

$$\text{Real}: \qquad \xi_1 c_1 + b_1 c_4 = a_1 + \xi_2 c_2 \tag{2.3}$$

$$\text{Imaginary}: \qquad \xi_1 s_1 + b_1 s_4 = \xi_2 s_2 \tag{2.4}$$

Second loop closure equation is written as follows by considering the loop $A_1 - B_1 - B_3 - A_3 - A_1$:

$$\overrightarrow{A_1B_1} + \overrightarrow{B_1B_3} = \overrightarrow{A_1A_3} + \overrightarrow{A_3B_3} \tag{2.5}$$

$$\xi_1 e^{i\theta_1} + b_2 e^{i(\theta_4+\beta)} = a_{2x} + ia_{2y} + \xi_3 e^{i\theta_3} \tag{2.6}$$

It is also possible to decompose Equation (2.6) into its real and imaginary parts in the same manner as done before for Equation (2.2):

$$\text{Real}: \qquad \xi_1 c_1 + b_2 c_{4''} = a_{2x} + \xi_3 c_3 \tag{2.7}$$

$$\text{Imaginary}: \qquad \xi_1 s_1 + b_2 s_{4''} = a_{2y} + \xi_3 s_3 \tag{2.8}$$

Define

$$\mathbf{q} = \begin{bmatrix} \theta_1 & \xi_1 & \theta_2 & \xi_2 & \theta_3 & \xi_3 & \theta_4 \end{bmatrix}^T \tag{2.9}$$

By differentiating Equations (2.3), (2.4) and (2.7), (2.8) one can obtain velocity level loop closure equations as follows:

$$\mathbf{J_c}\dot{\mathbf{q}} = \mathbf{0} \tag{2.10}$$

where

$$\mathbf{J_c} = \begin{bmatrix} -\xi_1 s_1 & c_1 & \xi_2 s_2 & -c_2 & 0 & 0 & -b_1 s_4 \\ \xi_1 c_1 & s_1 & -\xi_2 c_2 & -s_2 & 0 & 0 & b_1 c_4 \\ -\xi_1 s_1 & c_1 & 0 & 0 & \xi_3 s_3 & -c_3 & -b_2 s_{4''} \\ \xi_1 c_1 & s_1 & 0 & 0 & -\xi_3 c_3 & -s_3 & b_2 c_{4''} \end{bmatrix} \tag{2.11}$$

Position vector of the end-point P can be written as follows:

$$\overrightarrow{A_1P} = \overrightarrow{A_1B_1} + \overrightarrow{B_1P} \tag{2.12}$$

Let x_p and y_p be the x and y coordinates of the end-point, respectively. Then, Equation (2.12) can be rewritten in complex form as:

$$x_P + iy_P = \xi_1 e^{i\theta_1} + b_3 e^{i(\theta_4+\gamma)} \tag{2.13}$$

By separating real and imaginary parts of Equation (2.13), and noting that $\theta_4 = \theta_4$ position level task equations can be obtained as follows:

$$x_P = \xi_1 c_1 + b_3 c_{4'''} \tag{2.14}$$

$$y_P = \xi_1 s_1 + b_3 s_{4'''} \tag{2.15}$$

$$\theta_4 = \theta_4 \tag{2.16}$$

Velocity of the end-point P can be obtained by differentiating Equations (2.14)-(2.16):

$$\mathbf{J_t}\dot{\mathbf{q}} = \dot{\mathbf{X}} \tag{2.17}$$

where

$$\mathbf{J_t} = \begin{bmatrix} -\xi_1 s_1 & c_1 & 0 & 0 & 0 & 0 & -b_3 s_{4'''} \\ \xi_1 c_1 & s_1 & 0 & 0 & 0 & 0 & b_3 c_{4'''} \\ 0 & 0 & 0 & 0 & 0 & 0 & 1 \end{bmatrix} \tag{2.18}$$

and

$$\mathbf{X} = \begin{bmatrix} x_P & y_P & \theta_4 \end{bmatrix}^T \tag{2.19}$$

By following [13,14], one can combine Equations (2.10) and (2.17) as:

$$\mathbf{J}\dot{\mathbf{q}} = \mathbf{h} \tag{2.20}$$

where

$$\mathbf{J} = \begin{bmatrix} \mathbf{J_c} \\ \mathbf{J_t} \end{bmatrix} \tag{2.21}$$

and

$$\mathbf{h} = \begin{bmatrix} \mathbf{0} \\ \dot{\mathbf{X}} \end{bmatrix} \tag{2.22}$$

In order to obtain the acceleration level kinematic relations, one can simply differentiate Equation (2.20).

$$\dot{\mathbf{J}}\dot{\mathbf{q}} + \mathbf{J}\ddot{\mathbf{q}} = \dot{\mathbf{h}} \tag{2.23}$$

Equation (2.23) can be solved for $\ddot{\mathbf{q}}$ as follows:

$$\ddot{\mathbf{q}} = \mathbf{J}^{-1}\left(-\dot{\mathbf{J}}\dot{\mathbf{q}} + \dot{\mathbf{h}}\right) \tag{2.24}$$

where

$$\dot{\mathbf{J}} = \begin{bmatrix} \dot{J}_{11} & \dot{J}_{12} & \dot{J}_{13} & \dot{J}_{14} & 0 & 0 & \dot{J}_{17} \\ \dot{J}_{21} & \dot{J}_{22} & \dot{J}_{23} & \dot{J}_{24} & 0 & 0 & \dot{J}_{27} \\ \dot{J}_{31} & 0 & 0 & 0 & \dot{J}_{35} & \dot{J}_{36} & \dot{J}_{37} \\ \dot{J}_{41} & 0 & 0 & 0 & \dot{J}_{45} & \dot{J}_{46} & \dot{J}_{47} \\ \dot{J}_{51} & 0 & 0 & 0 & 0 & 0 & \dot{J}_{57} \\ \dot{J}_{61} & 0 & 0 & 0 & 0 & 0 & \dot{J}_{67} \\ 0 & 0 & 0 & 0 & 0 & 0 & 0 \end{bmatrix} \tag{2.25}$$

Elements of $\dot{\mathbf{J}}$ are as follows:

$$\dot{J}_{11} = \dot{J}_{31} = \dot{J}_{51} = -\dot{\xi}_1 s_1 - \xi_1 \dot{\theta}_1 c_1 \tag{2.26}$$

$$\dot{J}_{21} = \dot{J}_{41} = \dot{J}_{61} = \dot{\xi}_1 c_1 - \xi_1 \dot{\theta}_1 s_1 \tag{2.27}$$

$$\dot{J}_{12} = \dot{J}_{14} = \dot{\theta}_2 s_2 \tag{2.28}$$

$$\dot{J}_{22} = \dot{J}_{24} = -\dot{\theta}_2 c_2 \tag{2.29}$$

$$\dot{J}_{13} = \dot{\xi}_2 s_2 + \xi_2 \dot{\theta}_2 c_2 \tag{2.30}$$

$$\dot{J}_{23} = -\dot{\xi}_2 c_2 + \xi_2 \dot{\theta}_2 s_2 \tag{2.31}$$

$$\dot{J}_{35} = \dot{\xi}_3 s_3 + \xi_3 \dot{\theta}_3 c_3 \tag{2.32}$$

$$\dot{J}_{45} = -\dot{\xi}_3 c_3 + \xi_3 \dot{\theta}_3 s_3 \tag{2.33}$$

$$\dot{J}_{36} = \dot{\theta}_3 s_3 \tag{2.34}$$

$$\dot{J}_{46} = -\dot{\theta}_3 c_3 \tag{2.35}$$

$$\dot{J}_{17} = -b_1 \dot{\theta}_4 c_4 \tag{2.36}$$

$$\dot{J}_{27} = -b_1 \dot{\theta}_4 s_4 \tag{2.37}$$

$$\dot{J}_{37} = -b_2 \dot{\theta}_4 c_{4''} \tag{2.38}$$

$$\dot{J}_{47} = -b_2 \dot{\theta}_4 s_{4''} \tag{2.39}$$

$$\dot{J}_{57} = -b_3 \dot{\theta}_4 c_{4'''} \tag{2.40}$$

$$\dot{J}_{67} = -b_3 \dot{\theta}_4 s_{4'''} \tag{2.41}$$

As apparent from Equation (2.24), singularities arise when

$$\left|\mathbf{J}\right| = -\xi_1 \xi_2 \xi_3 = 0 \tag{2.42}$$

These singularities are of Type I [13, 14]. They correspond to cases where the length of any of the legs of the robot becomes zero. Such a case is not physically possible, so Type I and Type III singularities are not taken into account in this study.

2.2. Dynamic Analysis

The Lagrangian method will be used to formulate the dynamics of the robot. General form of the Lagrangian equations can be written as below:

$$\tau_i = \frac{d}{dt}\left(\frac{\partial L}{\partial \dot{q}_i}\right) - \frac{\partial L}{\partial q_i} \tag{2.43}$$

where τ_i stands for the generalized actuator force or torque at the joint whose joint variable is q_i , and L is the Lagrangian given by

$$L = K - V \tag{2.44}$$

Here, K and V are the total kinetic and potential energies of the system, respectively.

In order to obtain the Lagrangian, one can start by writing the position vector of mass center of each moving link in complex form:

$$\mathbf{r}_{\mathbf{G_1}} = g_1 c_1 + i g_1 s_1 \tag{2.45}$$

$$\mathbf{r}_{\mathbf{G_2}} = (\xi_1 - g_2) c_1 + i(\xi_1 - g_2) s_1 \tag{2.46}$$

$$\mathbf{r}_{\mathbf{G_3}} = g_3 c_2 + i g_3 s_2 \tag{2.47}$$

$$\mathbf{r}_{\mathbf{G_4}} = (\xi_2 - g_4) c_2 + i(\xi_2 - g_4) s_2 \tag{2.48}$$

$$\mathbf{r}_{\mathbf{G_5}} = g_5 c_3 + i g_5 s_3 \tag{2.49}$$

$$\mathbf{r}_{\mathbf{G_6}} = (\xi_3 - g_6) c_3 + i(\xi_3 - g_6) s_3 \tag{2.50}$$

$$\mathbf{r}_{\mathbf{G_7}} = \xi_1 c_1 + g_7 c_{4'} + i\left(\xi_1 s_1 + g_7 s_{4'}\right) \tag{2.51}$$

Differentiating Equations (2.45)-(2.51), one can obtain mass center velocities. These velocities will be needed to find the kinetic energy of each link.

$$\mathbf{V}_{\mathbf{G_1}} = -\dot{\theta}_1 g_1 s_1 + i\dot{\theta}_1 g_1 c_1 \tag{2.52}$$

$$\mathbf{V}_{\mathbf{G_2}} = \dot{\xi}_1 c_1 - \left(\xi_1 - g_2\right)\dot{\theta}_1 s_1 + i\left(\dot{\xi}_1 s_1 + \left(\xi_1 - g_2\right)\dot{\theta}_1 c_1\right) \tag{2.53}$$

$$\mathbf{V}_{\mathbf{G_3}} = -\dot{\theta}_2 g_3 s_2 + i\dot{\theta}_2 g_3 c_2 \tag{2.54}$$

$$\mathbf{V}_{\mathbf{G_4}} = \dot{\xi}_2 c_2 - \left(\xi_2 - g_4\right)\dot{\theta}_2 s_2 + i\left(\dot{\xi}_2 s_2 + \left(\xi_2 - g_4\right)\dot{\theta}_2 c_2\right) \tag{2.55}$$

$$\mathbf{V}_{\mathbf{G_5}} = -\dot{\theta}_3 g_5 s_3 + i\dot{\theta}_3 g_5 c_3 \tag{2.56}$$

$$\mathbf{V}_{\mathbf{G_6}} = \dot{\xi}_3 c_3 - \left(\xi_3 - g_6\right)\dot{\theta}_3 s_3 + i\left(\dot{\xi}_3 s_3 + \left(\xi_3 - g_6\right)\dot{\theta}_3 c_3\right) \tag{2.57}$$

$$\mathbf{V}_{\mathbf{G_7}} = \dot{\xi}_1 c_1 - \dot{\theta}_1 \xi_1 s_1 - \dot{\theta}_4 g_7 s_{4'} + i\left(\dot{\xi}_1 s_1 + \dot{\theta}_1 \xi_1 c_1 + \dot{\theta}_4 g_7 c_{4'}\right) \tag{2.58}$$

In order to obtain the kinetic energy of each link, the squares of the magnitudes of the above velocity vectors should be found. They are obtained as follows:

$$V_{G_1}^2 = \dot{\theta}_1^2 g_1^2 \tag{2.59}$$

$$V_{G_2}^2 = \dot{\xi}_1^2 + \left(\xi_1 - g_2\right)^2 \dot{\theta}_1^2 \tag{2.60}$$

$$V_{G_3}^2 = \dot{\theta}_2^2 g_3^2 \tag{2.61}$$

$$V_{G_4}^2 = \dot{\xi}_2^2 + \left(\xi_2 - g_4\right)^2 \dot{\theta}_2^2 \tag{2.62}$$

$$V_{G_5}^2 = \dot{\theta}_3^2 g_5^2 \tag{2.63}$$

$$V_{G_6}^2 = \dot{\xi}_3^2 + \left(\xi_3 - g_6\right)^2 \dot{\theta}_3^2 \tag{2.64}$$

$$V_{G_7}^2 = \dot{\xi}_1^2 + \dot{\theta}_1^2\xi_1^2 + \dot{\theta}_4^2 g_7^2 + 2\dot{\xi}_1\dot{\theta}_4 g_7 s_{14'} + 2\dot{\theta}_1\dot{\theta}_4\xi_1 g_7 c_{14'} \tag{2.65}$$

Then the Lagrangian function for the open-tree system is written as:

$$\begin{aligned} L = {} & \frac{1}{2}m_1\dot{\theta}_1^2 g_1^2 + \frac{1}{2}I_1\dot{\theta}_1^2 + \frac{1}{2}m_2\left(\dot{\xi}_1^2 + \left(\xi_1 - g_2\right)^2\dot{\theta}_1^2\right) + \frac{1}{2}I_2\dot{\theta}_1^2 + \frac{1}{2}m_3\dot{\theta}_2^2 g_3^2 \\ & + \frac{1}{2}I_3\dot{\theta}_2^2 + \frac{1}{2}m_4\left(\dot{\xi}_2^2 + \left(\xi_2 - g_4\right)^2\dot{\theta}_2^2\right) + \frac{1}{2}I_4\dot{\theta}_2^2 + \frac{1}{2}m_5\dot{\theta}_3^2 g_5^2 + \frac{1}{2}I_5\dot{\theta}_3^2 \\ & + \frac{1}{2}m_6\left(\dot{\xi}_3^2 + \left(\xi_3 - g_6\right)^2\dot{\theta}_3^2\right) + \frac{1}{2}I_6\dot{\theta}_3^2 \\ & + \frac{1}{2}m_7\left(\dot{\xi}_1^2 + \dot{\theta}_1^2\xi_1^2 + \dot{\theta}_4^2 g_7^2 + 2\dot{\xi}_1\dot{\theta}_4 g_7 s_{14'} + 2\dot{\theta}_1\dot{\theta}_4\xi_1 g_7 c_{14'}\right) \\ & + \frac{1}{2}I_7\dot{\theta}_4^2 - m_1 g g_1 s_1 - m_2 g\left(\xi_1 - g_2\right)s_1 - m_3 g g_3 s_2 - m_4 g\left(\xi_2 - g_4\right)s_2 - m_5 g g_5 s_3 \\ & - m_6 g\left(\xi_3 - g_6\right)s_3 - m_7 g\left(\xi_1 s_1 + g_7 s_{4'}\right) \end{aligned} \tag{2.66}$$

In the following part, the equations of motion will be derived for the open-tree system. The equation of motion associated with $q_i = \theta_1$ can be obtained step by step as follows:

$$\frac{d}{dt}\left(\frac{\partial L}{\partial \dot{\theta}_1}\right) - \frac{\partial L}{\partial \theta_1} = 0 \tag{2.67}$$

$$\frac{\partial L}{\partial \theta_1} = m_7\left(\dot{\xi}_1\dot{\theta}_4 g_7 c_{14'} - \dot{\theta}_1\dot{\theta}_4\xi_1 g_7 s_{14'}\right) - m_1 g g_1 c_1 - m_2 g\left(\xi_1 - g_2\right)c_1 - m_7 g\xi_1 c_1 \tag{2.68}$$

$$\frac{\partial L}{\partial \dot{\theta}_1} = m_1\dot{\theta}_1 g_1^2 + I_1\dot{\theta}_1 + m_2\dot{\theta}_1\left(\xi_1 - g_2\right)^2 + m_7\left(\dot{\theta}_1\xi_1^2 + \dot{\theta}_4\xi_1 g_7 c_{14'}\right) + I_2\dot{\theta}_1 \tag{2.69}$$

$$\begin{aligned} \frac{d}{dt}\left(\frac{\partial L}{\partial \dot{\theta}_1}\right) = {} & \ddot{\theta}_1\left(m_1 g_1^2 + I_1 + I_2 + m_2\left(\xi_1 - g_2\right)^2 + m_7\xi_1^2\right) \\ & + 2m_2\dot{\theta}_1\dot{\xi}_1\left(\xi_1 - g_2\right) + m_7\dot{\xi}_1\left(2\dot{\theta}_1\xi_1 + \dot{\theta}_4 g_7 c_{14'}\right) + \ddot{\theta}_4 m_7\xi_1 g_7 c_{14'} \\ & - m_7\left(\dot{\theta}_1 - \dot{\theta}_4\right)\left(\dot{\theta}_4\xi_1 g_7 s_{14'}\right) \end{aligned} \tag{2.70}$$

$$\ddot{\theta}_1\left(m_1 g_1^2 + I_1 + I_2 + m_2\left(\xi_1 - g_2\right)^2 + m_7\xi_1^2\right) + 2m_2\dot{\theta}_1\dot{\xi}_1\left(\xi_1 - g_2\right) + 2m_7\dot{\xi}_1\dot{\theta}_1\xi_1 \\ +\ddot{\theta}_4 m_7\xi_1 g_7 c_{14'} + m_7\dot{\theta}_4^2\xi_1 g_7 s_{14'} + m_1 g g_1 c_1 + m_2 g\left(\xi_1 - g_2\right)c_1 + m_7 g\xi_1 c_1 = 0 \tag{2.71}$$

Equation of motion associated with $q_i = \xi_1$ is derived by using the Lagrangian method below.

$$\frac{d}{dt}\left(\frac{\partial L}{\partial\dot{\xi}_1}\right) - \frac{\partial L}{\partial\xi_1} = F_1 \tag{2.72}$$

$$\frac{\partial L}{\partial\xi_1} = m_2\dot{\theta}_1^2\left(\xi_1 - g_2\right) + m_7\left(\dot{\theta}_1^2\xi_1 + \dot{\theta}_1\dot{\theta}_4 g_7 c_{14'}\right) - m_2 g s_1 - m_7 g s_1 \tag{2.73}$$

$$\frac{\partial L}{\partial\dot{\xi}_1} = m_2\dot{\xi}_1 + m_7\left(\dot{\xi}_1 + \dot{\theta}_4 g_7 s_{14'}\right) \tag{2.74}$$

$$\frac{d}{dt}\left(\frac{\partial L}{\partial\dot{\xi}_1}\right) = \ddot{\xi}_1\left(m_2 + m_7\right) + \ddot{\theta}_4 m_7 g_7 s_{14'} + m_7\left(\dot{\theta}_1 - \dot{\theta}_4\right)\dot{\theta}_4 g_7 c_{14'} \tag{2.75}$$

$$\ddot{\xi}_1\left(m_2 + m_7\right) + \ddot{\theta}_4 m_7 g_7 s_{14'} - m_7\dot{\theta}_4^2 g_7 c_{14'} - m_2\dot{\theta}_1^2\left(\xi_1 - g_2\right) - m_7\dot{\theta}_1^2\xi_1 + m_2 g s_1 \\ +m_7 g s_1 = F_1 \tag{2.76}$$

Equation of motion associated with $q_i = \theta_2$ is obtained below.

$$\frac{d}{dt}\left(\frac{\partial L}{\partial\dot{\theta}_2}\right) - \frac{\partial L}{\partial\theta_2} = 0 \tag{2.77}$$

$$\frac{\partial L}{\partial\theta_2} = -m_3 g g_3 c_2 - m_4 g\left(\xi_2 - g_4\right)c_2 \tag{2.78}$$

$$\frac{\partial L}{\partial\dot{\theta}_2} = m_3\dot{\theta}_2 g_3^2 + I_3\dot{\theta}_2 + m_4\dot{\theta}_2\left(\xi_2 - g_4\right)^2 + I_4\dot{\theta}_2 \tag{2.79}$$

$$\frac{d}{dt}\left(\frac{\partial L}{\partial\dot{\theta}_2}\right) = \ddot{\theta}_2\left(m_3 g_3^2 + I_3 + I_4 + m_4\left(\xi_2 - g_4\right)^2\right) + 2m_4\dot{\theta}_2\dot{\xi}_2\left(\xi_2 - g_4\right) \tag{2.80}$$

$$\ddot{\theta}_2\left(m_3 g_3^2 + I_3 + I_4 + m_4\left(\xi_2 - g_4\right)^2\right) + 2m_4\dot{\theta}_2\dot{\xi}_2\left(\xi_2 - g_4\right) + m_3 g g_3 c_2 + m_4 g\left(\xi_2 - g_4\right)c_2 = 0 \tag{2.81}$$

Equation of motion associated with $q_i = \xi_2$ can be derived as:

$$\frac{d}{dt}\left(\frac{\partial L}{\partial \dot{\xi}_2}\right) - \frac{\partial L}{\partial \xi_2} = F_2 \tag{2.82}$$

$$\frac{\partial L}{\partial \xi_2} = m_4\dot{\theta}_2^2\left(\xi_2 - g_4\right) - m_4 g s_2 \tag{2.83}$$

$$\frac{\partial L}{\partial \dot{\xi}_2} = m_4\dot{\xi}_2 \tag{2.84}$$

$$\frac{d}{dt}\left(\frac{\partial L}{\partial \dot{\xi}_2}\right) = \ddot{\xi}_2 m_4 \tag{2.85}$$

$$\ddot{\xi}_2 m_4 - m_4\dot{\theta}_2^2\left(\xi_2 - g_4\right) + m_4 g s_2 = F_2 \tag{2.86}$$

The derivation of equation of motion associated with $q_i = \theta_3$ is given below.

$$\frac{d}{dt}\left(\frac{\partial L}{\partial \dot{\theta}_3}\right) - \frac{\partial L}{\partial \theta_3} = 0 \tag{2.87}$$

$$\frac{\partial L}{\partial \theta_3} = -m_5 g g_5 c_3 - m_6 g\left(\xi_3 - g_6\right)c_3 \tag{2.88}$$

$$\frac{\partial L}{\partial \dot{\theta}_3} = m_5\dot{\theta}_3 g_5^2 + I_5\dot{\theta}_3 + m_6\dot{\theta}_3\left(\xi_3 - g_6\right)^2 + I_6\dot{\theta}_3 \tag{2.89}$$

$$\frac{d}{dt}\left(\frac{\partial L}{\partial \dot{\theta}_3}\right) = \ddot{\theta}_3\left(m_5 g_5^2 + I_5 + I_6 + m_6\left(\xi_3 - g_6\right)^2\right) + 2m_6\dot{\theta}_3\dot{\xi}_3\left(\xi_3 - g_6\right) \tag{2.90}$$

$$\ddot{\theta}_3\left(m_5 g_5^2 + I_5 + I_6 + m_6\left(\xi_3 - g_6\right)^2\right) + 2m_6\dot{\theta}_3\dot{\xi}_3\left(\xi_3 - g_6\right) + m_5 g g_5 c_3 + m_6 g\left(\xi_3 - g_6\right)c_3 = 0 \tag{2.91}$$

Equation of motion associated with $q_i = \xi_3$ can be determined as:

$$\frac{d}{dt}\left(\frac{\partial L}{\partial \dot{\xi}_3}\right) - \frac{\partial L}{\partial \xi_3} = F_3 \tag{2.92}$$

$$\frac{\partial L}{\partial \xi_3} = m_6\dot{\theta}_3^2\left(\xi_3 - g_6\right) - m_6 g s_3 \tag{2.93}$$

$$\frac{\partial L}{\partial \dot{\xi}_3} = m_6\dot{\xi}_3 \tag{2.94}$$

$$\frac{d}{dt}\left(\frac{\partial L}{\partial \dot{\xi}_3}\right) = \ddot{\xi}_3 m_6 \tag{2.95}$$

$$\ddot{\xi}_3 m_6 - m_6\dot{\theta}_3^2\left(\xi_3 - g_6\right) + m_6 g s_3 = F_3 \tag{2.96}$$

Finally, equation of motion associated with $q_i = \theta_4$ is obtained as follows:

$$\frac{d}{dt}\left(\frac{\partial L}{\partial \dot{\theta}_4}\right) - \frac{\partial L}{\partial \theta_4} = 0 \tag{2.97}$$

$$\frac{\partial L}{\partial \theta_4} = m_7\left(\dot{\theta}_1\dot{\theta}_4\xi_1 g_7 s_{14'} - \dot{\xi}_1\dot{\theta}_4 g_7 c_{14'}\right) - m_7 g g_7 c_{4'} \tag{2.98}$$

$$\frac{\partial L}{\partial \dot{\theta}_4} = m_7\left(\dot{\theta}_4 g_7^2 + \dot{\xi}_1 g_7 s_{14'} + \dot{\theta}_1\xi_1 g_7 c_{14'}\right) + I_7\dot{\theta}_4 \tag{2.99}$$

$$\frac{d}{dt}\left(\frac{\partial L}{\partial \dot{\theta}_4}\right) = \ddot{\theta}_4\left(m_7 g_7^2 + I_7\right) + m_7\left(\ddot{\xi}_1 g_7 s_{14'} + \left(\dot{\theta}_1 - \dot{\theta}_4\right)\dot{\xi}_1 g_7 c_{14'} + \ddot{\theta}_1\xi_1 g_7 c_{14'} + \dot{\theta}_1\dot{\xi}_1 g_7 c_{14'} + \left(\dot{\theta}_4 - \dot{\theta}_1\right)\dot{\theta}_1\xi_1 g_7 s_{14'}\right) \tag{2.100}$$

$$\ddot{\theta}_4\left(m_7 g_7^2 + I_7\right) + m_7\left(\ddot{\xi}_1 g_7 s_{14'} + \ddot{\theta}_1 \xi_1 g_7 c_{14'} + 2\dot{\theta}_1 \dot{\xi}_1 g_7 c_{14'} - \dot{\theta}_1^2 \xi_1 g_7 s_{14'}\right) + m_7 g g_7 c_{4'} = 0 \quad (2.101)$$

Equations of motion of this manipulator are coupled. For the purpose of finding the forward or inverse dynamics solution, these equations can be better expressed in matrix form. The equations of motion of the open-tree system can be expressed in matrix form as follows:

$$\mathbf{M}\ddot{\mathbf{q}} + \mathbf{N} = \mathbf{F} \quad (2.102)$$

where

$$\mathbf{M} = \begin{bmatrix} M_{11} & 0 & 0 & 0 & 0 & 0 & M_{17} \\ 0 & M_{22} & 0 & 0 & 0 & 0 & M_{27} \\ 0 & 0 & M_{33} & 0 & 0 & 0 & 0 \\ 0 & 0 & 0 & M_{44} & 0 & 0 & 0 \\ 0 & 0 & 0 & 0 & M_{55} & 0 & 0 \\ 0 & 0 & 0 & 0 & 0 & M_{66} & 0 \\ M_{71} & M_{72} & 0 & 0 & 0 & 0 & M_{77} \end{bmatrix} \quad (2.103)$$

$$\mathbf{N} = \begin{bmatrix} N_1 \\ N_2 \\ N_3 \\ N_4 \\ N_5 \\ N_6 \\ N_7 \end{bmatrix} \quad (2.104)$$

and

$$\mathbf{F} = \begin{bmatrix} 0 \\ F_1 \\ 0 \\ F_2 \\ 0 \\ F_3 \\ 0 \end{bmatrix} \tag{2.105}$$

The elements of $\mathbf{M}$ and $\mathbf{N}$ appearing above are given as:

$$M_{11} = m_1 g_1^2 + I_1 + I_2 + m_2 \left(\xi_1 - g_2\right)^2 + m_7 \xi_1^2 \tag{2.106}$$

$$M_{17} = m_7 \xi_1 g_7 c_{14'} \tag{2.107}$$

$$N_1 = 2m_2 \dot{\theta}_1 \dot{\xi}_1 \left(\xi_1 - g_2\right) + 2m_7 \dot{\xi}_1 \dot{\theta}_1 \xi_1 + m_7 \dot{\theta}_4^2 \xi_1 g_7 s_{14'} + m_1 g g_1 c_1 + m_2 g \left(\xi_1 - g_2\right) c_1 + m_7 g \xi_1 c_1 \tag{2.108}$$

$$M_{22} = m_2 + m_7 \tag{2.109}$$

$$M_{27} = m_7 g_7 s_{14'} \tag{2.110}$$

$$N_2 = -m_7 \dot{\theta}_4^2 g_7 c_{14'} - m_2 \dot{\theta}_1^2 \left(\xi_1 - g_2\right) - m_7 \dot{\theta}_1^2 \xi_1 + m_2 g s_1 + m_7 g s_1 \tag{2.111}$$

$$M_{33} = m_3 g_3^2 + I_3 + I_4 + m_4 \left(\xi_2 - g_4\right)^2 \tag{2.112}$$

$$N_3 = 2m_4 \dot{\theta}_2 \dot{\xi}_2 \left(\xi_2 - g_4\right) + m_3 g g_3 c_2 + m_4 g \left(\xi_2 - g_4\right) c_2 \tag{2.113}$$

$$M_{44} = m_4 \tag{2.114}$$

$$N_4 = -m_4 \dot{\theta}_2^2 \left(\xi_2 - g_4\right) + m_4 g s_2 \tag{2.115}$$

$$M_{55} = m_5 g_5^2 + I_5 + I_6 + m_6 \left(\xi_3 - g_6\right)^2 \tag{2.116}$$

$$N_5 = 2m_6\dot{\theta}_3\dot{\xi}_3\left(\xi_3 - g_6\right) + m_5 g g_5 c_3 + m_6 g\left(\xi_3 - g_6\right)c_3 \tag{2.117}$$

$$M_{66} = m_6 \tag{2.118}$$

$$N_6 = -m_6\dot{\theta}_3^2\left(\xi_3 - g_6\right) + m_6 g s_3 \tag{2.119}$$

$$M_{71} = m_7\xi_1 g_7 c_{14'} \tag{2.120}$$

$$M_{72} = m_7 g_7 s_{14'} \tag{2.121}$$

$$M_{77} = m_7 g_7^2 + I_7 \tag{2.122}$$

$$N_7 = m_7 g_7\left(2\dot{\theta}_1\dot{\xi}_1 c_{14'} - \dot{\theta}_1^2\xi_1 s_{14'} + g c_{4'}\right) \tag{2.123}$$

The equations of motion of the closed-loop mechanism can then be written as:

$$\mathbf{M\ddot{q}} + \mathbf{N} = \mathbf{F} + \mathbf{J_c^T\lambda} \tag{2.124}$$

where $\boldsymbol{\lambda} = \begin{bmatrix}\lambda_1 & \lambda_2 & \lambda_3 & \lambda_4\end{bmatrix}^T$ is the vector of Lagrange multipliers.

By following [13,14], the right-hand side of Equation (2.124) can be rearranged as:

$$\mathbf{A\mu} = \mathbf{F} + \mathbf{J_c^T\lambda} \tag{2.125}$$

where

$$\mathbf{A} = \begin{bmatrix} 0 & 0 & 0 & -\xi_1 s_1 & \xi_1 c_1 & -\xi_1 s_1 & \xi_1 c_1 \\ 1 & 0 & 0 & c_1 & s_1 & c_1 & s_1 \\ 0 & 0 & 0 & \xi_2 s_2 & -\xi_2 c_2 & 0 & 0 \\ 0 & 1 & 0 & -c_2 & -s_2 & 0 & 0 \\ 0 & 0 & 0 & 0 & 0 & \xi_3 s_3 & -\xi_3 c_3 \\ 0 & 0 & 1 & 0 & 0 & -c_3 & -s_3 \\ 0 & 0 & 0 & -b_1 s_4 & b_1 c_4 & -b_2 s_{4"} & b_2 c_{4"} \end{bmatrix} \tag{2.126}$$

and

$$\boldsymbol{\mu} = \begin{bmatrix} F_1 \\ F_2 \\ F_3 \\ \lambda_1 \\ \lambda_2 \\ \lambda_3 \\ \lambda_4 \end{bmatrix} \tag{2.127}$$

Following References [13, 14], it can be noticed that Type II singularities occur when

$$|\mathbf{A}| = \xi_1\xi_2\xi_3\left(b_1 s_{13} s_{42} + b_2 s_{12} s_{34''}\right) = 0 \tag{2.128}$$

Since it is not physically possible for ξ_1, ξ_2, ξ_3 to be zero as mentioned before, one can conclude that a Type II singularity is encountered when:

$$b_1 s_{13} s_{42} + b_2 s_{12} s_{34''} = 0 \tag{2.129}$$

The required linear actuator forces and Lagrangian multipliers are found by using the following equation.

$$\boldsymbol{\mu} = \mathbf{A}^{-1}\left(\mathbf{M}\ddot{\mathbf{q}} + \mathbf{N}\right) \tag{2.130}$$

Expanding Equation (2.130) leads to:

$$\begin{aligned} F_1 = \frac{1}{|\mathbf{A}|}\Big(& \xi_2\xi_3\left(b_1 c_{13} s_{42} + b_2 c_{12} s_{34''}\right)\left(M_{11}\ddot{\theta}_1 + M_{17}\ddot{\theta}_4 + N_1\right) \\ & -\xi_1\xi_2\xi_3\left(b_1 s_{24} s_{31} + b_2 s_{21} s_{34''}\right)\left(M_{22}\ddot{\xi}_1 + M_{27}\ddot{\theta}_4 + N_2\right) \\ & +\xi_1\xi_3\left(b_1 s_{43} + b_2 s_{34''}\right)\left(M_{33}\ddot{\theta}_2 + N_3\right) + \xi_1\xi_2\left(b_1 s_{42} + b_2 s_{24''}\right)\left(M_{55}\ddot{\theta}_3 + N_5\right) \\ & -\xi_1\xi_2\xi_3 s_{32}\left(M_{71}\ddot{\theta}_1 + M_{72}\ddot{\xi}_1 + M_{77}\ddot{\theta}_4 + N_7\right)\Big) \end{aligned} \tag{2.131}$$

$$
\begin{aligned}
F_2 = \frac{1}{|\mathbf{A}|}\Big(& -\xi_2\xi_3 b_2 s_{34''}\left(M_{11}\ddot{\theta}_1 + M_{17}\ddot{\theta}_4 + N_1\right) - \xi_1\xi_3\left(b_1 s_{13} c_{24} + b_2 c_{12} s_{34''}\right)\left(M_{33}\ddot{\theta}_2 + N_3\right) \\
& -\xi_1\xi_2\xi_3\left(b_1 s_{13} s_{24} + b_2 s_{21} s_{34''}\right)\left(M_{44}\ddot{\xi}_2 + N_4\right) - \xi_1\xi_2 b_2 s_{14''}\left(M_{55}\ddot{\theta}_3 + N_5\right) \\
& +\xi_1\xi_2\xi_3 s_{31}\left(M_{71}\ddot{\theta}_1 + M_{72}\ddot{\xi}_1 + M_{77}\ddot{\theta}_4 + N_7\right)\Big)
\end{aligned}
\tag{2.132}
$$

$$
\begin{aligned}
F_3 = \frac{1}{|\mathbf{A}|}\Big(& -\xi_2\xi_3 b_1 s_{42}\left(M_{11}\ddot{\theta}_1 + M_{17}\ddot{\theta}_4 + N_1\right) - \xi_1\xi_3 b_1 s_{41}\left(M_{33}\ddot{\theta}_2 + N_3\right) \\
& -\xi_1\xi_2\left(b_1 c_{13} s_{42} + b_2 s_{21} c_{34''}\right)\left(M_{55}\ddot{\theta}_3 + N_5\right) \\
& -\xi_1\xi_2\xi_3\left(b_1 s_{31} s_{42} + b_2 s_{21} s_{34''}\right)\left(M_{66}\ddot{\xi}_3 + N_6\right) \\
& -\xi_1\xi_2\xi_3 s_{21}\left(M_{71}\ddot{\theta}_1 + M_{72}\ddot{\xi}_1 + M_{77}\ddot{\theta}_4 + N_7\right)\Big)
\end{aligned}
\tag{2.133}
$$

Hence as shown in Equations (2.131)-(2.133) the required actuator forces tend to infinity when $|\mathbf{A}|$ becomes zero.

3. APPLICATION OF THE BALANCING METHOD

In this chapter, the singularity robust balancing method [18] will be applied to the robot. Figure 3.1 shows a balanced 3-RPR mechanism with three counterweights. Counterweights are placed close to the base in order to decrease their inertial loads.

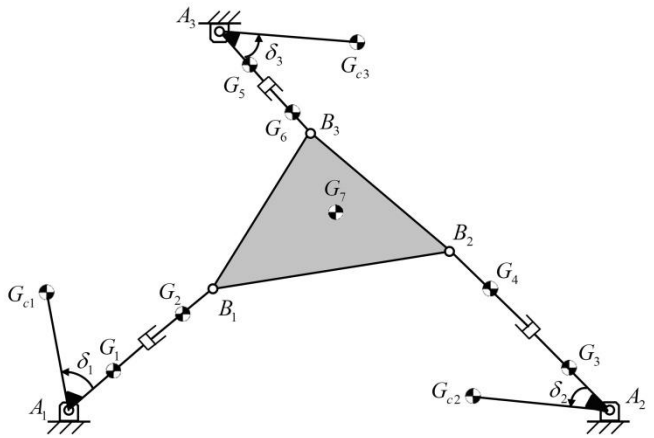

Figure 3.1 A balanced 3-RPR mechanism

Three counterweights with masses m_{c1}, m_{c2}, m_{c3} and centroidal moments of inertia I_{c1}, I_{c2}, I_{c3} are considered in this study. The mass center location of each counterweight is given by $r_1 = A_1G_{c1}$, $r_2 = A_2G_{c2}$, $r_3 = A_3G_{c3}$.

3.1. Dynamic Equations of Motion of the Balanced Robot

In order to determine the additional terms that will appear in the dynamic equations due to the counterweights, one can start by writing position vectors of their mass centers in complex forms as follows:

$$\mathbf{r_{c1}} = r_1\cos\left(\theta_1+\delta_1\right) + r_1\sin\left(\theta_1+\delta_1\right)i \tag{3.1}$$

$$\mathbf{r_{c2}} = r_2\cos\left(\theta_2+\delta_2\right) + r_2\sin\left(\theta_2+\delta_2\right)i \tag{3.2}$$

$$\mathbf{r_{c3}} = r_3 \cos\left(\theta_3 + \delta_3\right) + r_3 \sin\left(\theta_3 + \delta_3\right) i \tag{3.3}$$

By differentiating Equations (3.1)-(3.3), velocities of the centers of masses of the counterweights can be obtained. By obtaining these velocities, the change in the kinetic energy of the system caused by the counterweights can be found.

$$\mathbf{V_{c1}} = -r_1\dot{\theta}_1 \sin\left(\theta_1 + \delta_1\right) + r_1\dot{\theta}_1 \cos\left(\theta_1 + \delta_1\right) i \tag{3.4}$$

$$\mathbf{V_{c2}} = -r_2\dot{\theta}_2 \sin\left(\theta_2 + \delta_2\right) + r_2\dot{\theta}_2 \cos\left(\theta_2 + \delta_2\right) i \tag{3.5}$$

$$\mathbf{V_{c3}} = -r_3\dot{\theta}_3 \sin\left(\theta_3 + \delta_3\right) + r_3\dot{\theta}_3 \cos\left(\theta_3 + \delta_3\right) i \tag{3.6}$$

By using Equations (3.4)-(3.6), one can obtain the squares of the velocities of counterweight mass centers:

$$V_{c1}^2 = \dot{\theta}_1^2 r_1^2 \tag{3.7}$$

$$V_{c2}^2 = \dot{\theta}_2^2 r_2^2 \tag{3.8}$$

$$V_{c3}^2 = \dot{\theta}_3^2 r_3^2 \tag{3.9}$$

The change in the Lagrangian can be expressed as:

$$\Delta L = \Delta K - \Delta V \tag{3.10}$$

Here, ΔK represents the change in the kinetic energy of the system due to the counterweights.

$$\Delta K = \frac{1}{2} m_{c1} \dot{\theta}_1^2 r_1^2 + \frac{1}{2} I_{c1} \dot{\theta}_1^2 + \frac{1}{2} m_{c2} \dot{\theta}_2^2 r_2^2 + \frac{1}{2} I_{c2} \dot{\theta}_2^2 + \frac{1}{2} m_{c3} \dot{\theta}_3^2 r_3^2 + \frac{1}{2} I_{c3} \dot{\theta}_3^2 \tag{3.11}$$

The change in the potential energy of the system, ΔV, can be expressed as:

$$\Delta V = g m_{c1} r_1 \sin\left(\theta_1 + \delta_1\right) + g m_{c2} r_2 \sin\left(\theta_2 + \delta_2\right) + g m_{c3} r_3 \sin\left(\theta_3 + \delta_3\right) \tag{3.12}$$

Substituting Equations (3.11) and (3.12) into Equation (3.10) gives:

$$\begin{aligned}\Delta L = &\frac{1}{2}m_{c1}\dot{\theta}_1^2 r_1^2 + \frac{1}{2}I_{c1}\dot{\theta}_1^2 + \frac{1}{2}m_{c2}\dot{\theta}_2^2 r_2^2 + \frac{1}{2}I_{c2}\dot{\theta}_2^2 + \frac{1}{2}m_{c3}\dot{\theta}_3^2 r_3^2 + \frac{1}{2}I_{c3}\dot{\theta}_3^2 \\ &- gm_{c1}r_1\sin(\theta_1+\delta_1) - gm_{c2}r_2\sin(\theta_2+\delta_2) - gm_{c3}r_3\sin(\theta_3+\delta_3)\end{aligned} \tag{3.13}$$

The additional terms in the equation of motion associated with $q_i = \theta_1$ can then be found as described below.

Let

$$\Delta_1 = \frac{d}{dt}\left(\frac{\partial \Delta L}{\partial \dot{\theta}_1}\right) - \frac{\partial \Delta L}{\partial \theta_1} \tag{3.14}$$

Then,

$$\frac{\partial \Delta L}{\partial \theta_1} = -gm_{c1}r_1\cos(\theta_1+\delta_1) \tag{3.15}$$

$$\frac{\partial \Delta L}{\partial \dot{\theta}_1} = m_{c1}\dot{\theta}_1 r_1^2 + I_{c1}\dot{\theta}_1 \tag{3.16}$$

$$\frac{d}{dt}\left(\frac{\partial \Delta L}{\partial \dot{\theta}_1}\right) = \ddot{\theta}_1\left(m_{c1}r_1^2 + I_{c1}\right) \tag{3.17}$$

Thus,

$$\Delta_1 = \ddot{\theta}_1\left(m_{c1}r_1^2 + I_{c1}\right) + gm_{c1}r_1\cos(\theta_1+\delta_1) \tag{3.18}$$

The additional terms to be added to equation of motion associated with $q_i = \theta_2$ can be found as shown below.

$$\frac{\partial \Delta L}{\partial \theta_2} = -gm_{c2}r_2\cos(\theta_2+\delta_2) \tag{3.19}$$

$$\frac{\partial \Delta L}{\partial \dot{\theta}_2} = m_{c2}\dot{\theta}_2 r_2^2 + I_{c2}\dot{\theta}_2 \tag{3.20}$$

$$\frac{d}{dt}\left(\frac{\partial \Delta L}{\partial \dot{\theta}_2}\right) = \ddot{\theta}_2\left(m_{c2}r_2^2 + I_{c2}\right) \tag{3.21}$$

$$\begin{aligned}\Delta_3 &= \frac{d}{dt}\left(\frac{\partial \Delta L}{\partial \dot{\theta}_2}\right) - \frac{\partial \Delta L}{\partial \theta_2} \\ &= \ddot{\theta}_2\left(m_{c2}r_2^2 + I_{c2}\right) + gm_{c2}r_2\cos\left(\theta_2 + \delta_2\right)\end{aligned} \tag{3.22}$$

Lastly, the additional terms that will be added to equation of motion associated with $q_i = \theta_3$ is obtained below.

$$\frac{\partial \Delta L}{\partial \theta_3} = -gm_{c3}r_3\cos\left(\theta_3 + \delta_3\right) \tag{3.23}$$

$$\frac{\partial \Delta L}{\partial \dot{\theta}_3} = m_{c3}\dot{\theta}_3 r_3^2 + I_{c3}\dot{\theta}_3 \tag{3.24}$$

$$\frac{d}{dt}\left(\frac{\partial \Delta L}{\partial \dot{\theta}_3}\right) = \ddot{\theta}_3\left(m_{c3}r_3^2 + I_{c3}\right) \tag{3.25}$$

$$\begin{aligned}\Delta_5 &= \frac{d}{dt}\left(\frac{\partial \Delta L}{\partial \dot{\theta}_3}\right) - \frac{\partial \Delta L}{\partial \theta_3} \\ &= \ddot{\theta}_3\left(m_{c3}r_3^2 + I_{c3}\right) + gm_{c3}r_3\cos\left(\theta_3 + \delta_3\right)\end{aligned} \tag{3.26}$$

The dynamic equations of the balanced mechanism can then be expressed as:

$$\mathbf{M}\ddot{\mathbf{q}} + \mathbf{N} + \boldsymbol{\Delta} = \mathbf{A}\boldsymbol{\mu} \tag{3.27}$$

where $\boldsymbol{\Delta}$ is given by

$$\boldsymbol{\Delta} = \begin{bmatrix}\Delta_1 & \Delta_2 & \Delta_3 & \Delta_4 & \Delta_5 & \Delta_6 & \Delta_7\end{bmatrix}^T \tag{3.28}$$

Recall that Δ_1, Δ_3 and Δ_5 are already obtained in Equations (3.18), (3.22) and (3.26), respectively.

Since ΔL includes neither $\xi_1, \xi_2, \xi_3, \theta_4$, nor their derivatives, $\Delta_2 = \Delta_4 = \Delta_6 = \Delta_7 = 0$. Hence,

$$\mathbf{\Lambda} = \begin{bmatrix} \ddot{\theta}_1\left(m_{c1}r_1^2 + I_{c1}\right) + gm_{c1}r_1\cos\left(\theta_1 + \delta_1\right) \\ 0 \\ \ddot{\theta}_2\left(m_{c2}r_2^2 + I_{c2}\right) + gm_{c2}r_2\cos\left(\theta_2 + \delta_2\right) \\ 0 \\ \ddot{\theta}_3\left(m_{c3}r_3^2 + I_{c3}\right) + gm_{c3}r_3\cos\left(\theta_3 + \delta_3\right) \\ 0 \\ 0 \end{bmatrix} \tag{3.29}$$

3.2. Derivation of the Balance Design Equation

First of all, rank deficiency of matrix $\mathbf{A}$ at a singular configuration should be determined. Let v be the rank deficiency of matrix $\mathbf{A}$ at the singular position. If $\frac{d^v}{dt^v}|\mathbf{A}| = 0$ then, in addition to the satisfaction of the consistency conditions [13,14], some high order conditions should be satisfied [17]. Recall that matrix $\mathbf{A}$ is already found in Equation (2.126).

It is obvious that rows 2, 4 and 6 of matrix $\mathbf{A}$ can never be linearly dependent with its other rows, so it will be sufficient to study the linear dependency relation among the rows of the below submatrix of $\mathbf{A}$ at the singularity:

$$\mathbf{A}^* = \begin{bmatrix} -\xi_1 s_1 & \xi_1 c_1 & -\xi_1 s_1 & \xi_1 c_1 \\ \xi_2 s_2 & -\xi_2 c_2 & 0 & 0 \\ 0 & 0 & \xi_3 s_3 & -\xi_3 c_3 \\ -b_1 s_4 & b_1 c_4 & -b_2 s_{4"} & b_2 c_{4"} \end{bmatrix} \tag{3.30}$$

Let the rank of $\mathbf{A}^*$ be 3 so, it is rank deficient by one at a Type II singularity. Suppose further that the following relation exists among its rows at this singularity:

$$C_1\mathbf{R_1} + C_2\mathbf{R_2} + C_3\mathbf{R_3} + C_4\mathbf{R_4} = \mathbf{0} \tag{3.31}$$

where $\mathbf{R_i}$ denotes the i 'th row of the $\mathbf{A}^*$ matrix and C_i are coefficients that are not all zero $(i=1,\cdots,4)$.

In this thesis, $\frac{d}{dt}|\mathbf{A}|$ is assumed to be nonzero at the singular position, so satisfying the consistency condition will be enough for passing through the singular configuration in a stable fashion [17]. Left-hand side of Equation (3.27) can be rewritten as:

$$\mathbf{W} = \mathbf{M}\ddot{\mathbf{q}} + \mathbf{N} + \boldsymbol{\Delta} \tag{3.32}$$

Similar to the partitioning of $\mathbf{A}$ as described above, only the first, third, fifth and seventh elements of the vector $\mathbf{W}$ will be considered since these rows correspond to the unactuated joint variables [18]. Let the $\mathbf{W}^*$ vector be a 4×1 vector that only consists of these elements of vector $\mathbf{W}$, i.e.,

$$\mathbf{W}^* = \begin{bmatrix} M_{11} & 0 & 0 & 0 & 0 & 0 & M_{17} \\ 0 & 0 & M_{33} & 0 & 0 & 0 & 0 \\ 0 & 0 & 0 & 0 & M_{55} & 0 & 0 \\ M_{71} & M_{72} & 0 & 0 & 0 & 0 & M_{77} \end{bmatrix} \begin{bmatrix} \ddot{\theta}_1 \\ \ddot{\xi}_1 \\ \ddot{\theta}_2 \\ \ddot{\xi}_2 \\ \ddot{\theta}_3 \\ \ddot{\xi}_3 \\ \ddot{\theta}_4 \end{bmatrix} + \begin{bmatrix} N_1 \\ N_3 \\ N_5 \\ N_7 \end{bmatrix} + \begin{bmatrix} \Delta_1 \\ \Delta_3 \\ \Delta_5 \\ \Delta_7 \end{bmatrix} \tag{3.33}$$

Let it be rewritten in a more compact form as follows:

$$\mathbf{W}^* = \begin{bmatrix} W_1^* \\ W_2^* \\ W_3^* \\ W_4^* \end{bmatrix} \tag{3.34}$$

where

$$W_1^* = \dot{\theta}_4^2 \xi_1 g_7 m_7 s_{14'} + \ddot{\theta}_1 \left(m_{c1} r_1^2 + I_{c1} \right) + \ddot{\theta}_1 \left(I_1 + I_2 + g_1^2 m_1 + \xi_1^2 m_7 + m_2 \left(\xi_1 - g_2 \right)^2 \right) + 2\dot{\theta}_1 \dot{\xi}_1 \left(\xi_1 m_7 + m_2 \left(\xi_1 - g_2 \right) \right) + m_{c1} r_1 g \cos\left(\delta_1 + \theta_1 \right) + g_1 m_1 g c_1 + \xi_1 m_7 g c_1 + m_2 g c_1 \left(\xi_1 - g_2 \right) + \ddot{\xi}_3 \xi_1 g_7 m_7 c_{14'} \quad (3.35)$$

$$W_2^* = \ddot{\theta}_2 \left(m_{c2} r_2^2 + I_{c2} \right) + \ddot{\theta}_3 \left(I_3 + I_4 + g_3^2 m_3 + m_4 \left(\xi_2 - g_4 \right)^2 \right) + m_{c2} r_2 g \cos\left(\delta_2 + \theta_2 \right) + 2\dot{\theta}_2 \dot{\xi}_2 m_4 \left(\xi_2 - g_4 \right) + g_3 m_3 g c_2 + m_4 g c_2 \left(\xi_2 - g_4 \right) \quad (3.36)$$

$$W_3^* = \ddot{\theta}_3 \left(m_{c3} r_3^2 + I_{c3} \right) + \ddot{\xi}_1 \left(I_5 + I_6 + g_5^2 m_5 + m_6 \left(\xi_3 - g_6 \right)^2 \right) + m_{c3} r_3 g \cos\left(\delta_3 + \theta_3 \right) + 2\dot{\theta}_3 \dot{\xi}_3 m_6 \left(\xi_3 - g_6 \right) + g_5 m_5 g c_3 + m_6 g c_3 \left(\xi_3 - g_6 \right) \quad (3.37)$$

$$W_4^* = \ddot{\xi}_3 \left(g_7^2 m_7 + I_7 \right) + g_7 m_7 \left(-\dot{\theta}_1^2 \xi_1 s_{14'} + 2\dot{\theta}_1 \dot{\xi}_1 c_{14'} + g c_{4'} \right) + \ddot{\theta}_2 g_7 m_7 s_{14'} + \ddot{\theta}_1 \xi_1 g_7 m_7 c_{14'} \quad (3.38)$$

Thus, the balance design equation to be satisfied for the singular configuration can be written as:

$$C_1 W_1^* + C_2 W_2^* + C_3 W_3^* + C_4 W_4^* = 0 \quad (3.39)$$

There are 12 independent parameters in balance design Equation (3.39). For simplifying the problem, the counterweights will be assumed to be applied such that

$$m_{c1} = m_{c2} = m_{c3} = m_c \quad (3.40)$$

$$r_1 = r_2 = r_3 = r \quad (3.41)$$

$$I_{c1} = I_{c2} = I_{c3} = I_c \quad (3.42)$$

$$\delta_1 = \delta_2 = \delta_3 = \delta \quad (3.43)$$

Then the balance design Equation (3.39) reduces to:

$$
\begin{aligned}
&\left(m_c r^2 + I_c\right)\left(C_1\ddot{\theta}_1 + C_2\ddot{\theta}_2 + C_3\ddot{\theta}_3\right) \\
&+\left(m_c rg\right)\left(C_1\cos\left(\delta+\theta_1\right) + C_2\cos\left(\delta+\theta_2\right) + C_3\cos\left(\delta+\theta_3\right)\right) \\
&+C_1\left(\dot{\theta}_4^2\xi_1 g_7 m_7 s_{14'} + \ddot{\theta}_1\left(I_1 + I_2 + g_1^2 m_1 + \xi_1^2 m_7 + m_2\left(\xi_1 - g_2\right)^2\right)\right. \\
&\left.+2\dot{\theta}_1\dot{\xi}_1\left(\xi_1 m_7 + m_2\left(\xi_1 - g_2\right)\right) + g_1 m_1 g c_1 + \xi_1 m_7 g c_1 + m_2 g c_1\left(\xi_1 - g_2\right) + \ddot{\xi}_3\xi_1 g_7 m_7 c_{14'}\right) \\
&+C_2\left(\ddot{\theta}_3\left(I_3 + I_4 + g_3^2 m_3 + m_4\left(\xi_2 - g_4\right)^2\right) + 2\dot{\theta}_2\dot{\xi}_2 m_4\left(\xi_2 - g_4\right) + g_3 m_3 g c_2\right. \\
&\left.+m_4 g c_2\left(\xi_2 - g_4\right)\right) \\
&+C_3\left(\ddot{\xi}_1\left(I_5 + I_6 + g_5^2 m_5 + m_6\left(\xi_3 - g_6\right)^2\right) + 2\dot{\theta}_3\dot{\xi}_3 m_6\left(\xi_3 - g_6\right) + g_5 m_5 g c_3\right. \\
&\left.+m_6 g c_3\left(\xi_3 - g_6\right)\right) \\
&+C_4\left(\ddot{\xi}_3\left(g_7^2 m_7 + I_7\right) + g_7 m_7\left(-\dot{\theta}_1^2\xi_1 s_{14'} + 2\dot{\theta}_1\dot{\xi}_1 c_{14'} + g c_{4'}\right) + \ddot{\theta}_2 g_7 m_7 s_{14'}\right. \\
&\left.+\ddot{\theta}_1\xi_1 g_7 m_7 c_{14'}\right) = 0
\end{aligned}
\tag{3.44}
$$

By rearranging trigonometric expressions,

$$
\begin{aligned}
&\left(m_c r^2 + I_c\right)\left(C_1\ddot{\theta}_1 + C_2\ddot{\theta}_2 + C_3\ddot{\theta}_3\right) \\
&+\left(m_c rg\right)\left(C_5\sin\left(\delta+\phi\right)\right) \\
&+C_1\left(\dot{\theta}_4^2\xi_1 g_7 m_7 s_{14'} + \ddot{\theta}_1\left(I_1 + I_2 + g_1^2 m_1 + \xi_1^2 m_7 + m_2\left(\xi_1 - g_2\right)^2\right)\right. \\
&\left.+2\dot{\theta}_1\dot{\xi}_1\left(\xi_1 m_7 + m_2\left(\xi_1 - g_2\right)\right) + g_1 m_1 g c_1 + \xi_1 m_7 g c_1 + m_2 g c_1\left(\xi_1 - g_2\right) + \ddot{\xi}_3\xi_1 g_7 m_7 c_{14'}\right) \\
&+C_2\left(\ddot{\theta}_3\left(I_3 + I_4 + g_3^2 m_3 + m_4\left(\xi_2 - g_4\right)^2\right) + 2\dot{\theta}_2\dot{\xi}_2 m_4\left(\xi_2 - g_4\right) + g_3 m_3 g c_2\right. \\
&\left.+m_4 g c_2\left(\xi_2 - g_4\right)\right) \\
&+C_3\left(\ddot{\xi}_1\left(I_5 + I_6 + g_5^2 m_5 + m_6\left(\xi_3 - g_6\right)^2\right) + 2\dot{\theta}_3\dot{\xi}_3 m_6\left(\xi_3 - g_6\right) + g_5 m_5 g c_3\right. \\
&\left.+m_6 g c_3\left(\xi_3 - g_6\right)\right) \\
&+C_4\left(\ddot{\xi}_3\left(g_7^2 m_7 + I_7\right) + g_7 m_7\left(-\dot{\theta}_1^2\xi_1 s_{14'} + 2\dot{\theta}_1\dot{\xi}_1 c_{14'} + g c_{4'}\right) + \ddot{\theta}_2 g_7 m_7 s_{14'}\right. \\
&\left.+\ddot{\theta}_1\xi_1 g_7 m_7 c_{14'}\right) = 0
\end{aligned}
\tag{3.45}
$$

where

$$
\phi = \operatorname{atan2}\left(-\frac{C_1 s_1 + C_2 s_2 + C_3 s_3}{C_1 c_1 + C_2 c_2 + C_3 c_3}\right) \tag{3.46}
$$

and

$$
C_5 = \sqrt{\left(C_1 c_1 + C_2 c_2 + C_3 c_3\right)^2 + \left(C_1 s_1 + C_2 s_2 + C_3 s_3\right)^2} \tag{3.47}
$$

In more compact form:

$$C_x\left(m_c r^2 + I_c\right) + C_y m_c r \sin\left(\delta + \phi\right) + C_z = 0 \tag{3.48}$$

where

$$C_x = C_1\ddot{\theta}_1 + C_2\ddot{\theta}_2 + C_3\ddot{\theta}_3 \tag{3.49}$$

$$C_y = C_5 \sin\left(\delta + \phi\right) \tag{3.50}$$

and

$$\begin{aligned} C_z = {} & C_1\left(\dot{\theta}_4^2\xi_1 g_7 m_7 s_{14'} + \ddot{\theta}_1\left(I_1 + I_2 + g_1^2 m_1 + \xi_1^2 m_7 + m_2\left(\xi_1 - g_2\right)^2\right)\right. \\ & + 2\dot{\theta}_1\dot{\xi}_1\left(\xi_1 m_7 + m_2\left(\xi_1 - g_2\right)\right) + g_1 m_1 g c_1 + \xi_1 m_7 g c_1 + m_2 g c_1\left(\xi_1 - g_2\right) + \ddot{\xi}_3\xi_1 g_7 m_7 c_{14'}\Big) \\ & + C_2\left(\ddot{\theta}_3\left(I_3 + I_4 + g_3^2 m_3 + m_4\left(\xi_2 - g_4\right)^2\right) + 2\dot{\theta}_2\dot{\xi}_2 m_4\left(\xi_2 - g_4\right) + g_3 m_3 g c_2\right. \\ & \left. + m_4 g c_2\left(\xi_2 - g_4\right)\right) \\ & + C_3\left(\ddot{\xi}_1\left(I_5 + I_6 + g_5^2 m_5 + m_6\left(\xi_3 - g_6\right)^2\right) + 2\dot{\theta}_3\dot{\xi}_3 m_6\left(\xi_3 - g_6\right) + g_5 m_5 g c_3\right. \\ & \left. + m_6 g c_3\left(\xi_3 - g_6\right)\right) \\ & + C_4\left(\ddot{\xi}_3\left(g_7^2 m_7 + I_7\right) + g_7 m_7\left(-\dot{\theta}_1^2\xi_1 s_{14'} + 2\dot{\theta}_1\dot{\xi}_1 c_{14'} + g c_{4'}\right) + \ddot{\theta}_2 g_7 m_7 s_{14'}\right. \\ & \left. + \ddot{\theta}_1\xi_1 g_7 m_7 c_{14'}\right) \end{aligned} \tag{3.51}$$

3.3. Consistent Positions of Counterweights

In this section possible counterweight locations will be determined. In order to do that, balance design Equation (3.48) will be examined.

Theorem 1: Consider a 3-RPR planar parallel robot as shown in Figure 2.1. Let the manipulator be balanced for crossing a Type II singular configuration using three identical counterweights, each being fixed identically to one separate leg as shown in Figure 3.1. Let further A be rank-deficient by one at this configuration. Suppose also that $\frac{d}{dt}|\mathbf{A}| \neq 0$ at the singularity time. Then, for a given desired motion, the consistent loci of each counterweight on the associated leg describe a circle centered at $x' = C_{y3}$, $y' = C_{y4}$ and having a radius of $\sqrt{C_{z1} + \frac{C_{x1}}{m_c} - \frac{I_c}{m_c}}$ where $A_i x' y'$ is the coordinate

system that is attached to that leg as shown in Figure 3.2, $x' = r\cos(\delta)$, $y' = r\sin(\delta)$, $C_{y3} = -C_y \sin(\phi)/(2C_x)$, $C_{y4} = -C_y \cos(\phi)/(2C_x)$, $C_{z1} = C_y^2/(4C_x^2)$ and $C_{x1} = -C_z/C_x$.

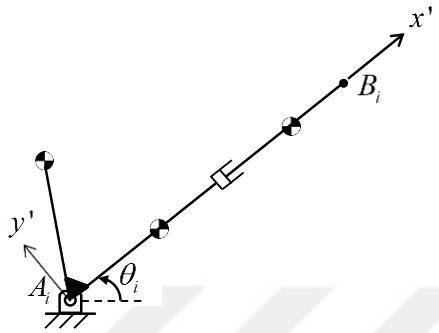

Figure 3.2 $x'-$ and $y'-$ axes where $i = 1,2,3$

Proof: In order to prove this theorem, Equation (3.48) should be rearranged as,

$$C_x r^2 + C_y r \sin(\delta + \phi) + \frac{C_z}{m_c} + \frac{C_x I_c}{m_c} = 0 \tag{3.52}$$

Expanding the trigonometric term in Equation (3.52) leads to;

$$C_x r^2 + C_{y1} r \cos(\delta) + C_{y2} r \sin(\delta) + C_z/m_c + C_x I_c/m_c = 0 \tag{3.53}$$

where

$$C_{y1} = C_y \sin(\phi) \tag{3.54}$$

and

$$C_{y2} = C_y \cos(\phi) \tag{3.55}$$

Equation (3.53) is the equation of a circle. In order to see this, recall that $x' = r\cos(\delta)$, $y' = r\sin(\delta)$ (see Figure 3.2). Then,

$$C_x\left(x'^2+y'^2\right)+C_{y1}x'+C_{y2}y'+C_z/m_c+C_xI_c/m_c=0 \tag{3.56}$$

$$x'^2-\left(-\frac{C_{y1}}{C_x}\right)x'+\left(\frac{C_{y1}}{2C_x}\right)^2+y'^2-\left(-\frac{C_{y2}}{C_x}\right)y'+\left(\frac{C_{y2}}{2C_x}\right)^2=\left(\frac{C_{y1}}{2C_x}\right)^2+\left(\frac{C_{y2}}{2C_x}\right)^2 -\frac{C_z}{C_xm_c}-\frac{I_c}{m_c} \tag{3.57}$$

$$x'^2-2C_{y3}x'+C_{y3}^2+y'^2-2C_{y4}y'+C_{y4}^2=C_{y3}^2+C_{y4}^2+\frac{C_{x1}}{m_c}-\frac{I_c}{m_c} \tag{3.58}$$

where

$$C_{y3}=-\frac{C_{y1}}{2C_x}=-C_y\sin(\phi)/(2C_x) \tag{3.59}$$

$$C_{y4}=-\frac{C_{y2}}{2C_x}=-C_y\cos(\phi)/(2C_x) \tag{3.60}$$

and

$$C_{x1}=-\frac{C_z}{C_x} \tag{3.61}$$

Then,

$$\left(x'-C_{y3}\right)^2+\left(y'-C_{y4}\right)^2=C_{z1}+\frac{C_{x1}}{m_c}-\frac{I_c}{m_c} \tag{3.62}$$

where

$$\mathrm{C}_{z1}=C_{y3}^2+C_{y4}^2=\frac{C_{y1}^2+C_{y2}^2}{4C_x^2}=\left(\frac{C_y}{2C_x}\right)^2 \tag{3.63}$$

Equation (3.62) is the equation of a circle centered at $x' = C_{y3}$, $y' = C_{y4}$ and having a radius of $\sqrt{C_{z1} + \frac{C_{x1}}{m_c} - \frac{I_c}{m_c}}$.

Corollary 1: For a singularity robust balancing to be possible, the following inequality should hold at the singularity.

$$\left| \frac{C_x \left(m_c r^2 + I_c \right) + C_z}{C_y m_c r} \right| \leq 1 \tag{3.64}$$

Proof: In order to prove this theorem, Equation (3.48) can be rearranged as:

$$\sin\left(\delta + \phi\right) = -\frac{C_x \left(m_c r^2 + I_c \right) + C_z}{C_y m_c r} \tag{3.65}$$

Since absolute value of the sine function can't be higher than 1, satisfying the balance design equation is not possible outside the given interval stated in the corollary.

Corollary 2: For a singularity robust balancing to be possible, the following inequality should hold at the singularity.

$$C_{z1} + \frac{C_{x1}}{m_c} - \frac{I_c}{m_c} > 0 \tag{3.66}$$

Proof: In Theorem 1, the radius of the circle that describes consistent positions of each of identical and identically located counterweights is given as

$$\rho = \sqrt{C_{z1} + \frac{C_{x1}}{m_c} - \frac{I_c}{m_c}} \tag{3.67}$$

In order to have a non-zero real radius, the inequality (3.66) should be satisfied.

Theorem 2: Under the conditions of Theorem 1, consistent loci of different counterweights on each leg describe concentric circles for a given desired motion as long as the conditions of Corollary 1 and Corollary 2 are satisfied.

Proof: The center of the circle of interest is located at $x' = C_{y3}$ and $y' = C_{y4}$. Since C_{y3} and C_{y4} expressions do not contain any counterweight parameter, center locations will be the same for consistent locations of different counterweights. However their radii are functions of counterweight mass and mass moment of inertia as given in Equation (3.67).

Note that similar conclusions were previously drawn by Özdemir [19,20] for proper payload locations of planar parallel robots passing through Type II singularities.

4. NUMERICAL EXAMPLE

Throughout the rest of the thesis, the numerical values provided in Table 4.1 are used for the robot parameters.

Table 4.1 Numerical values of the robot parameters

Parameter	Value	Parameter	Value	Parameter	Value
a_1	1 m	m_1 to m_6	0.05 kg	α	$\pi/6$
a_{2x}	0.5 m	m_7	0.1 kg	β	$\pi/3$
a_{2y}	1 m	I_1 to I_6	10^{-4} kg·m^2	γ	$\pi/9$
b_1, b_2	0.2 m	I_7	3×10^{-4} kg·m^2		
b_3	0.1 m	g_1 to g_6	0.5 m		
		g_7	$\sqrt{3}/2$ m		

4.1. Generating a Trajectory that Passes Through a Singular Point

Figure 4.1 shows the considered path.

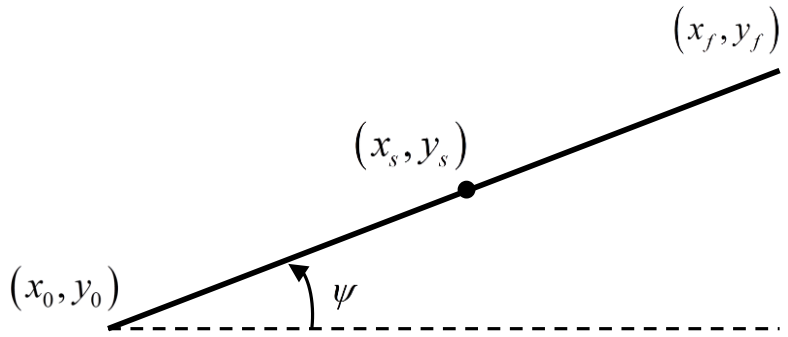

Figure 4.1 The path considered

Trajectories along x and y axes can be written as:

$$x(t) = x_0 + s(t)\cos(\psi) \tag{4.1}$$

$$y(t) = y_0 + s(t)\sin(\psi) \tag{4.2}$$

where t denotes time, $x_0 = 0.7767$ m, $y_0 = 0.6686$ m, $\psi = 45^o$, and the total length of the path is 0.02 m. The total duration of the task is $t_f = 10$ s.

The task requirements considered while generating the trajectory $s(t)$ are given in Table 4.2.

Table 4.2 Trajectory requirements

Initial Conditions	Final Conditions
$s(t=0) = 0$	$s(t=t_f) = 0.02$
$\dot{s}(t=0) = 0$	$\dot{s}(t=t_f) = 0$
$\ddot{s}(t=0) = 0$	$\ddot{s}(t=t_f) = 0$

The above requirements can be satisfied by using a fifth order polynomial for $s(t)$.

$$s(t) = z_5 t^5 + z_4 t^4 + z_3 t^3 + z_2 t^2 + z_1 t + z_0 \tag{4.3}$$

where

$$z_0 = 0 \tag{4.4}$$

$$z_1 = 0 \tag{4.5}$$

$$z_2 = 0 \tag{4.6}$$

$$z_3 = 0.2 \times 10^{-3} \tag{4.7}$$

$$z_4 = -0.3 \times 10^{-4} \tag{4.8}$$

$$z_5 = 1.2 \times 10^{-6} \tag{4.9}$$

Figure 4.2 shows the y versus x curve.

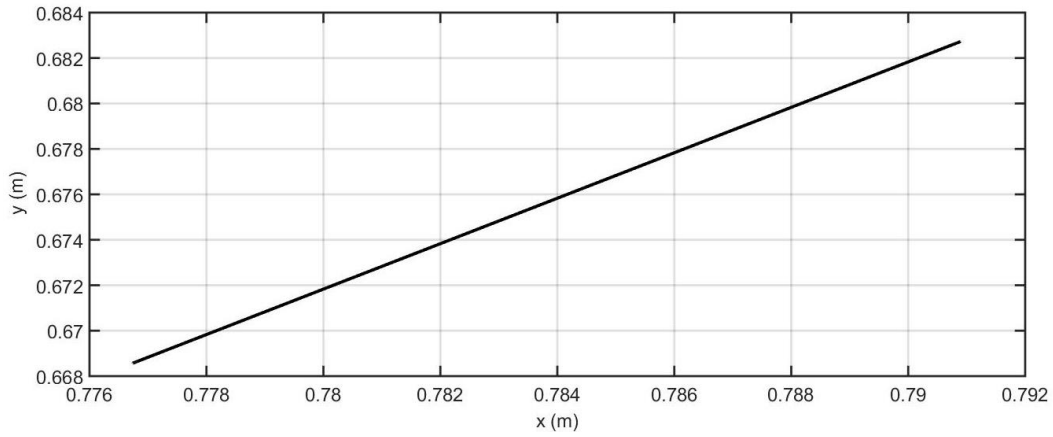

Figure 4.2 y versus x curve.

The end-point of the robot crosses a singular point with $x_s = 0.7838$ m, $y_s = 0.6756$ m at $t = 5$ s while this trajectory is realized.

4.2. Inverse Dynamics of the Unbalanced Robot

It can be seen that the required actuator forces for the robot to follow the prescribed trajectory grow unbounded near t = 5 s which is the singularity time. Hence the desired trajectory cannot be achieved by the unbalanced manipulator.

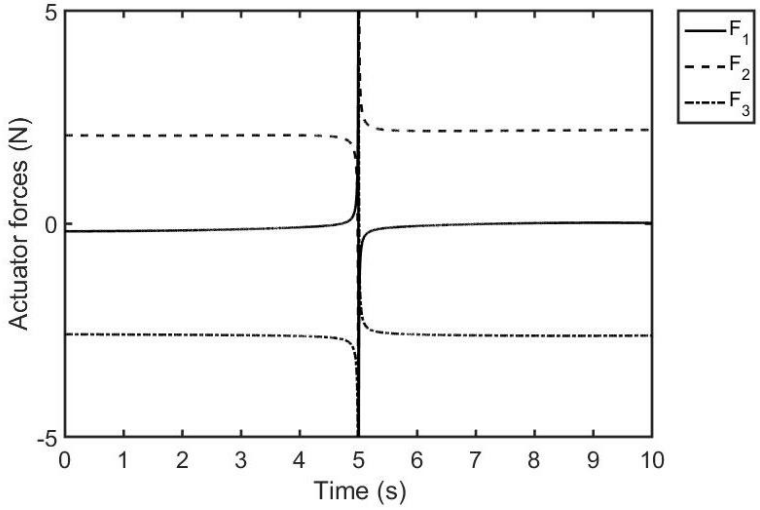

Figure 4.3 Required forces for the unbalanced system to realize the prescribed trajectory

4.3. Inverse Dynamics of the Balanced Robot

When the values of the model parameters and joint variables at the singularity are substituted, $\mathbf{A}^*$ matrix becomes:

$$\mathbf{A}^* = \begin{bmatrix} -0.6842 & 0.6842 & -0.6842 & 0.6842 \\ 0.6000 & 0.1344 & 0 & 0 \\ 0 & 0 & -0.2008 & 0.3478 \\ 0.0842 & 0.1814 & -0.1150 & 0.1636 \end{bmatrix} \tag{4.10}$$

Rank of $\mathbf{A}^*$ is 3 so, it is rank deficient by one. The following relation holds at the singularity.

$$C_1\mathbf{R_1} + C_2\mathbf{R_2} + C_3\mathbf{R_3} + C_4\mathbf{R_4} = \mathbf{0} \tag{4.11}$$

where $C_1 = -0.1941,\ C_2 = -0.3617,\ C_3 = 0.0886,\ C_4 = 1.$

For the considered trajectory, $\frac{d}{dt}|\mathbf{A}|$ is nonzero at the singularity time (see Figure 4.4) so satisfying the consistency condition will be sufficient for passing through the singular configuration in a stable fashion [17].

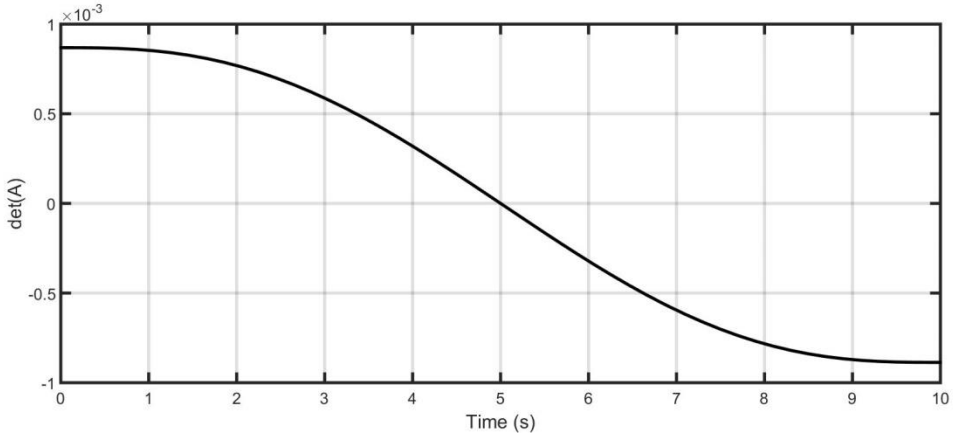

Figure 4.4 $|\mathbf{A}|$ versus time graph while the robot is following the given trajectory.

$\mathbf{W}^*$ is calculated at the singularity as:

$$\mathbf{W}^* = \begin{bmatrix} 1.0068 + 2.4760\left(m_{c1}r_1^2 + I_{c1}\right)\times 10^{-21} + 9.81 m_{c1} r_1 \cos\left(0.7854 + \delta_1\right) \\ -0.0659 + 0.3364\left(m_{c2}r_2^2 + I_{c2}\right)\times 10^{-4} + 9.81 m_{c2} r_2 \cos\left(1.7912 + \delta_2\right) \\ 0.1706 - 0.4359\left(m_{c3}r_3^2 + I_{c3}\right)\times 10^{-4} + 9.81 m_{c3} r_3 \cos\left(5.7596 + \delta_3\right) \\ 0.84620 \end{bmatrix} \tag{4.12}$$

It follows from Equation (3.39) that the balance design equation for this particular case is:

$$\begin{aligned} &0.6897 - 0.4806\left(m_{c1}r_1^2 + I_{c1}\right)\times 10^{-21} - 1.9041 m_{c1} r_1 \cos\left(0.7854 + \delta_1\right) \\ &-0.1217\left(m_{c2}r_2^2 + I_{c2}\right)\times 10^{-4} - 3.5483 m_{c2} r_2 \cos\left(1.7912 + \delta_2\right) \\ &-0.0386\left(m_{c3}r_3^2 + I_{c3}\right)\times 10^{-4} - 0.8692 m_{c3} r_3 \cos\left(5.7596 + \delta_3\right) = 0 \end{aligned} \tag{4.13}$$

or, if the counterweights are applied such that Equations (3.40)-(3.43) are satisfied, then it reduces to

$$0.6897 - 0.1603\left(m_c r^2 + I_c\right)\times 10^{-4} + 5.2464 m_c r \sin\left(0.03467 + \delta\right) = 0 \tag{4.14}$$

There are 4 different counterweight parameters in the above equation, and hence 6 different binary combinations of them can be examined. According to Equation (4.14), one balancing scenario can be selected as $\delta = 5\pi/4$, $I_c = 5\times 10^{-3}$, $m_c = 0.3596$, $r = 0.5$. The required actuator forces remain finite and continuous for this balanced robot, as shown in Figure 4.5.

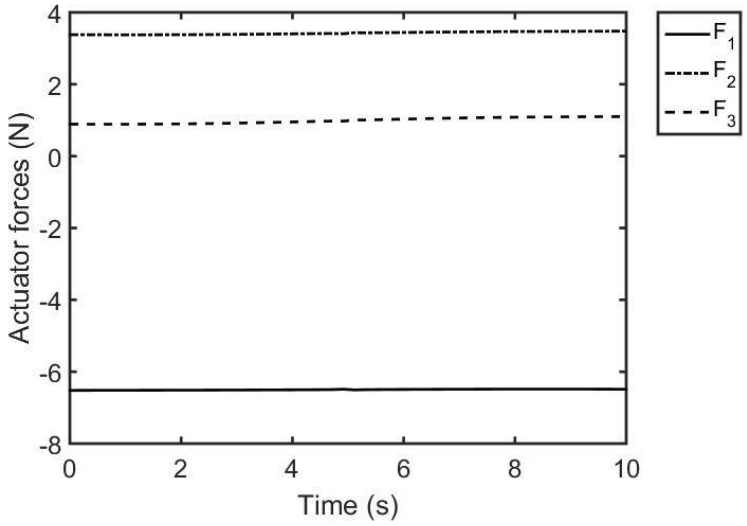

Figure 4.5 Required forces for the balanced system to follow the given trajectory.

In the following chapter, different balancing alternatives will be analyzed in more detail.

5. COMPARISON OF DIFFERENT BALANCING ALTERNATIVES

In order to compare different balancing alternatives, a measure that determines the effectiveness of the applied balancing is needed. This performance index is chosen as:

$$PI = \int_0^{t_f} \sum_{i=1}^{3} |F_i| dt \tag{5.1}$$

In Equation (5.1) PI stands for the performance index. For reducing the actuator efforts, the value of this index should be kept as low as possible.

5.1. Examination of the r versus m_c Relation

By examining the r versus m_c graph (Figure 5.1) one can conclude that the mass moments of inertia of the counterweights do not lead to dramatic changes in the suitable values of m_c and r for realizing the prescribed task. The reason of this is that the coefficient of I_c is in the order of 10^{-4} in Equation (4.14), but of course, effect of I_c can differ for different values of robot parameters or for different trajectories.

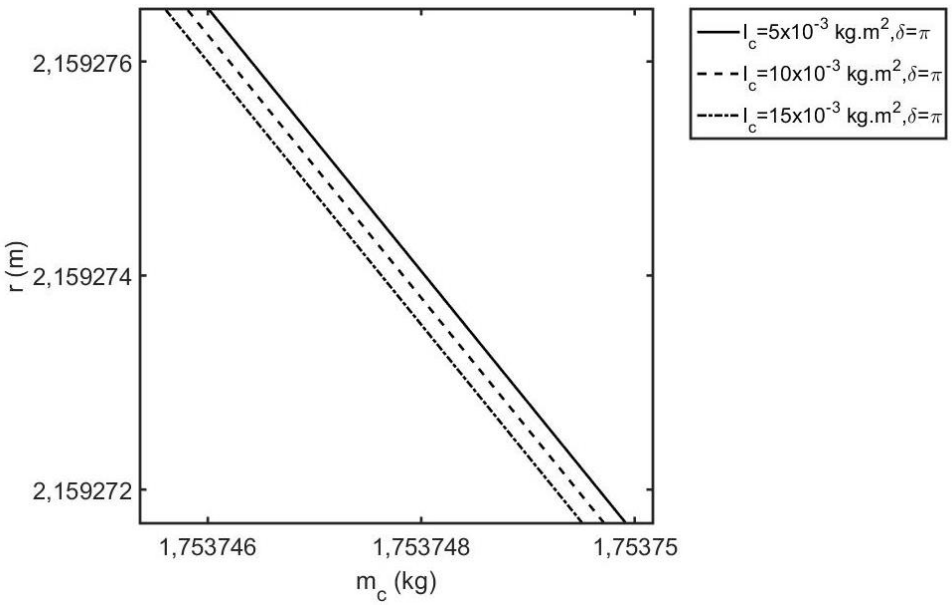

Figure 5.1 r vs. m_c for different I_c values

In the following analyses, I_c is taken as 5×10^{-3}kg.m^2 unless otherwise stated.

The curves that show the suitable r and m_c values for different δ values are plotted in Figure 5.2.

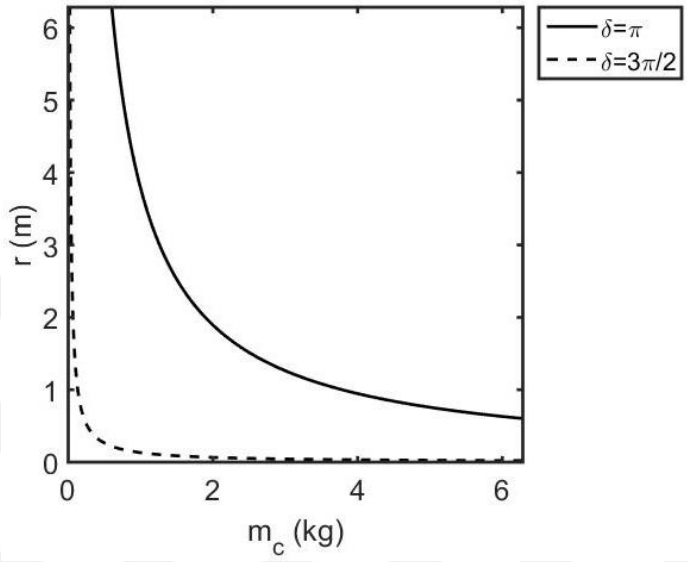

Figure 5.2 r vs. m_c for different δ values

Table 5.1 shows numerically calculated performance indices for some points seen in Figure 5.2:

Table 5.1 Performance indices for some points selected on Figure 5.2.

Case	δ (rad)	r (m)	m_c (kg)	Performance Index
1.1	π	4	0.9465	2117.3
1.2		3	1.2622	2101.2
1.3		1.9460	1.9460	2084.3
1.4		1.2624	3	2073.3
1.5		0.9468	4	2068.2
1.6	$\frac{3\pi}{2}$	2	0.06577	65.0411
1.7		0.75	0.1754	64.8214
1.8		0.3627	0.3627	64.7533
1.9		0.1754	0.75	64.7204
1.10		0.06577	2	64.7011

Table 5.1 suggests that for a given δ, the performance index does not change dramatically along each of these r versus m_c curves. It is also interesting to note that the value of the $m_c r$ product does not change substantially along each of the curves seen in Figure 5.2.

Another result that can be deduced from Table 5.1 is that performance index can change greatly for different values of δ. Performance index values for $\delta = \pi$ are approximately 30 times larger than $\delta = \frac{3\pi}{2}$, and this result shows that selection of counterweight locations is quite critical for the performance of the robot.

5.2. Examination of the δ versus I_c Relation

m_c and r are not seen alone in the balance design Equation (4.14), they are seen in $m_c r^2$ and $m_c r$ terms. Coefficient of the $m_c r^2$ term is pretty small when compared to those of the other terms as discussed in the previous section. Thus, the suitable values of

δ and I_c do not change dramatically for different m_c and r values as long as the value of the $m_c r$ product is kept the same.

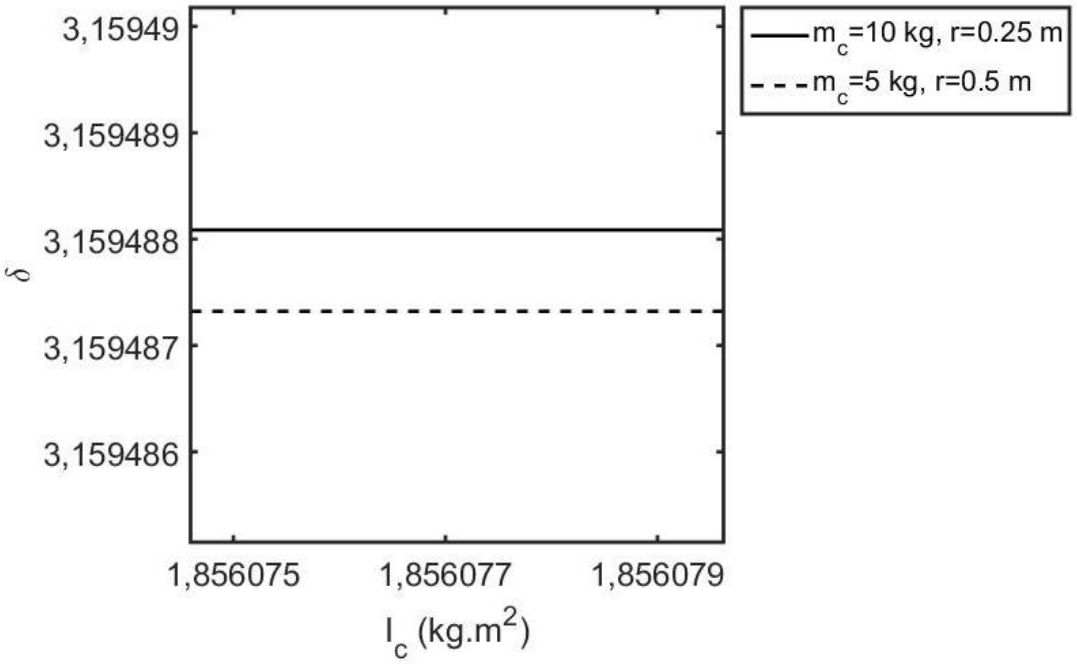

Figure 5.3 δ vs. I_c for different m_c and r values such that $m_c r$ is kept fixed

For this reason, the grouped parameter $m_c r$ will be used in the following analyses.

Figure 5.4a. and Figure 5.4b. show δ curves for different $m_c r$ values. As clearly seen, there are two solutions for δ for a given $m_c r$ value. Reason of this is that in Theorem 1, it is proven that possible loci of counterweights for a given m_c and I_c describe a circle. To find the δ values that correspond to a given m_c, I_c and r value, the problem can be solved geometrically by intersecting the consistent counterweight loci circle with another circle that is centered at A_1 and having a radius of r. In this particular case, these two circles intersect each other at two different points, so, there are two different solutions for δ for the same $m_c r$ value.

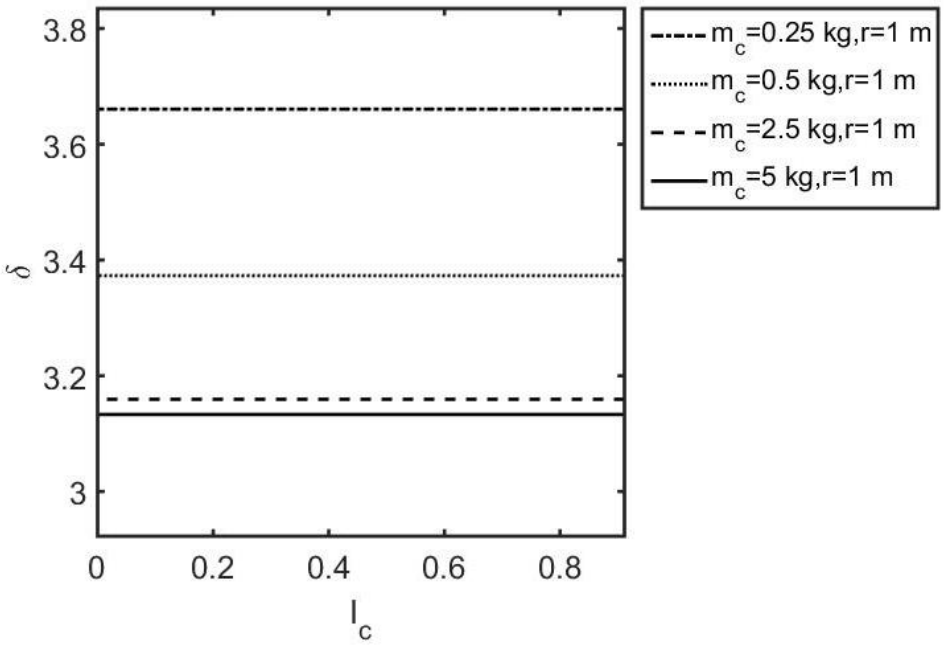

Figure 5.4a First solution for δ against I_c for different m_c values

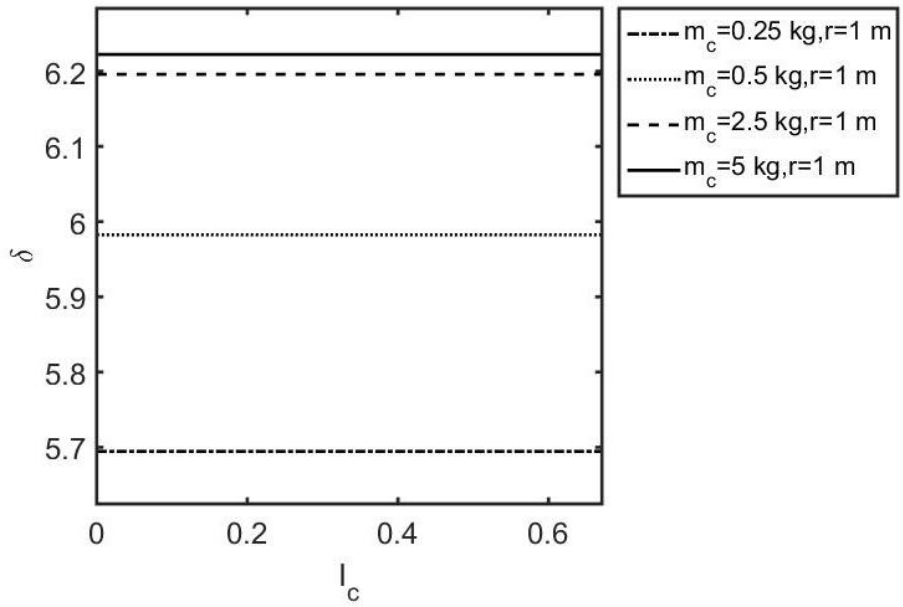

Figure 5.4b Second solution for δ against I_c for different m_c values

Table 5.2 Performance indices for some points selected on Figure 5.4a and Figure 5.4b

Case	$m_c r$ (kg.m)	δ (rad)	I_c (kg.m^2)	Performance Index
2.1	0.25	3.6607	5×10^{-3}	157.5
2.2	$(m_c = 0.25, r = 1)$	5.6948		96.5
2.3	0.5	3.3730		301.6
2.4	$(m_c = 0.5, r = 1)$	5.9825		209.9
2.5	2.5	3.1595		1375.2
2.6	$(m_c = 2.5, r = 1)$	6.1959		1268.4
2.7	5	3.1332		2713.3
2.8	$(m_c = 5, r = 1)$	6.2222		2586.1

By examining cases 2.5, 2.7 and 2.6, 2.8 the relation between $m_c r$ and the performance index is nearly linear for the interval $m_c r \geq 2.5$ (kg.m). Reason of this is that δ does not change dramatically in this interval and the coefficient of $m_c r^2$ is significantly less in absolute sense than that of $m_c r$ in the balance design equation (4.14), as previously mentioned.

5.3. Examination of the r versus δ Relation

First consistent counterweight positions are analyzed on the $x'y'-$ coordinate system.

When the aforementioned numerical values are substituted into Equation (3.62) and I_c is chosen as 5×10^{-3} kg.m^2, it is found that the consistent positions of counterweights are given by

$$(x'-0.5674)^2 + (y'-16.3544)^2 = 267.7866 + 4.3026/m_c \qquad (5.2)$$

Figure 5.5 shows the loci of counterweights of different masses that satisfy the balance design equation (4.14).

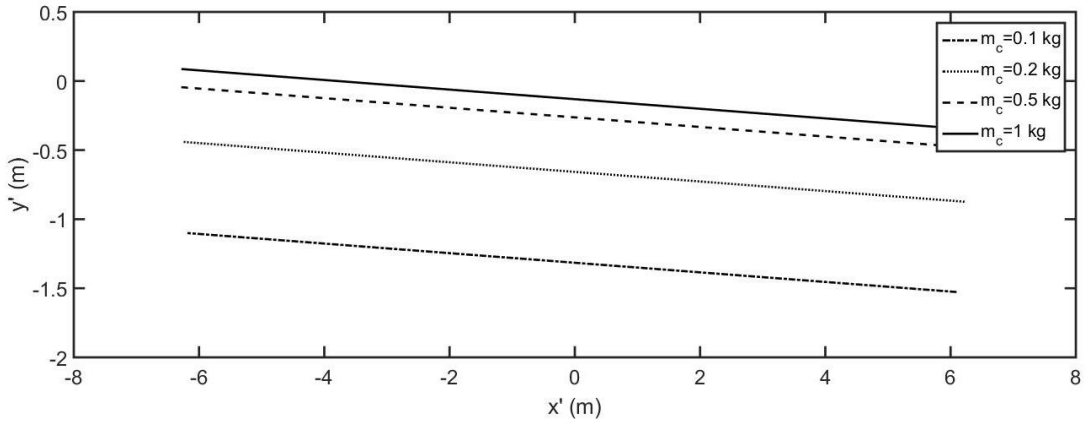

Figure 5.5 Consistent counterweight locations for different m_c values

Even though shapes in Figure 5.5 seem like parallel lines, they are concentric circles as proved in Theorem 2. These circles are so large that they look like parallel lines in this narrow range.

The curves of suitable r versus δ values for different m_c values are plotted in Figure 5.6.

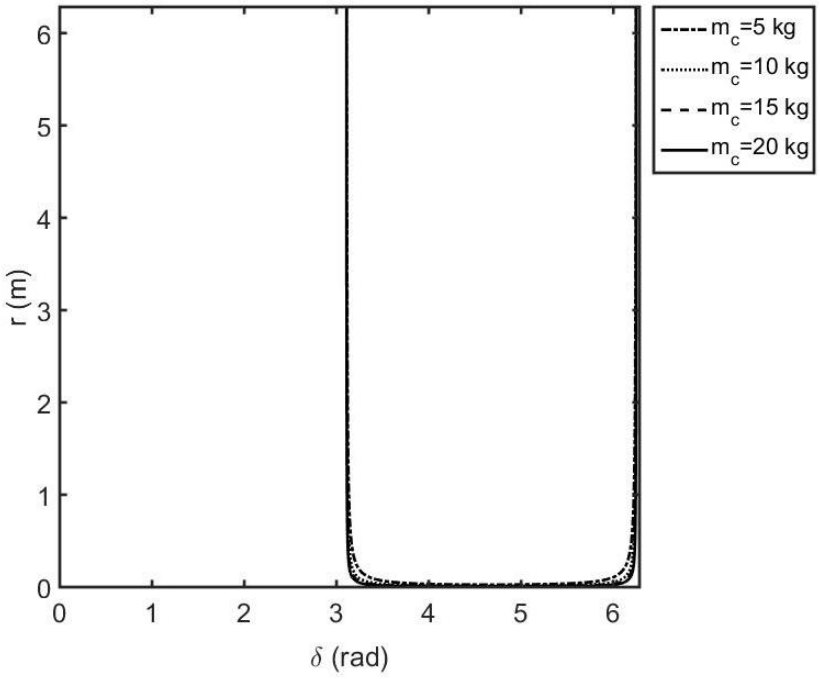

Figure 5.6 r vs. δ for different m_c values

In order to satisfy Equation (4.14), the sine function should have negative values for this numerical example. In this scenario, $m_c r^2$ value is not dominant so, this fact limits the values of δ to $3.1069<\delta<6.2485$. It can be seen from Figure 5.6 that the balance design equation (4.14) can't be satisfied for almost the first half of the range $0 \le \delta \le 2\pi$ (Figure 5.6).

Table 5.3 Performance indices for some points selected on Figure 5.6

Case	$m_c\ (\text{kg})$	$r\ (\text{m})$	$m_c r\ (\text{kg.m})$	$\delta\ (\text{rad})$	Performance Index
3.1	5	0.0264	0.1320	4.7685	63.2669
3.2		0.2124	1.0620	3.2310	603.4330
3.3		0.0623	0.3115	3.5426	193.5239
3.4		0.0342	0.1710	3.9852	101.5680
3.5		0.0291	0.1455	4.2321	77.8724
3.6	10	0.0132	0.1320	4.7685	63.2647
3.7		0.0149	0.1490	5.1623	52.2365
3.8		0.0167	0.1670	5.3455	52.0731
3.9		0.0272	0.2720	5.7432	106.9053
3.10		0.1092	1.0920	6.1278	530.3200

Examining Table 5.3 leads to the conclusion that, around $\delta = \pi$ and $\delta = 2\pi$, the performance index attains its highest values (case 3.2 and case 3.10), which is not desirable, and around the midpoint of this range, it has significantly lower values (cases 3.6-3.8).

Cases 3.1 and 3.6 verify the previously found result that for the same $m_c r$ values, the performance index does not change dramatically. Generally, the performance index increases with increasing $m_c r$ values. However, there is an exception to this (see cases 3.6 and 3.7).

5.4. Examination of the r versus I_c Relation

Family of r versus I_c curves for different m_c and δ values are plotted in Figure 5.7.

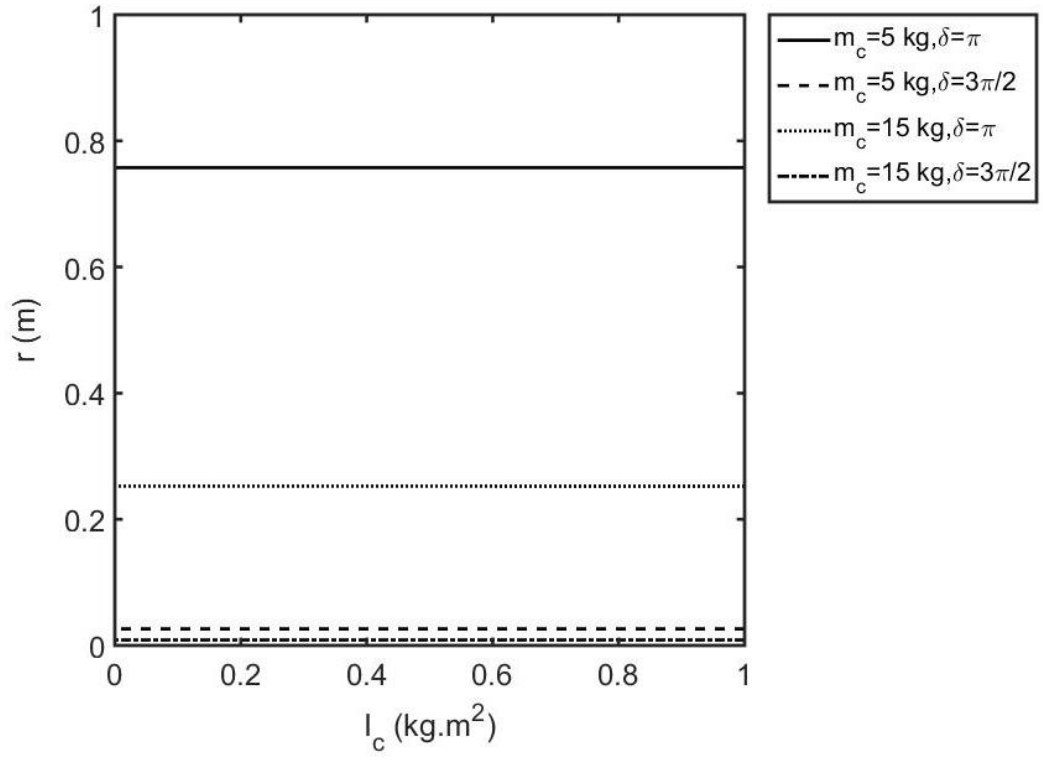

Figure 5.7 r vs. I_c for different m_c and δ pairs

By examining Figure 5.7, it is once again seen that effect of change of mass moment of inertia is not significant in the balance design equation for the selected values in the analysis.

Table 5.4 Performance indices for some points selected on Figure 5.7

Case	$m_c\,(\mathrm{kg})$	$\delta\ (\mathrm{rad})$	$r\ (\mathrm{m})$	Performance Index
4.1	5	π	0.7575	2065.2
4.2		$\frac{3\pi}{2}$	0.0263	64.6942
4.3	15	π	0.2525	2057.0
4.4		$\frac{3\pi}{2}$	0.00877	64.6911

Table 5.4 supports the previous conclusions. For cases 4.1 and 4.3 or 4.2 and 4.4, the $m_c r$ values are nearly the same and as a result of this, their performance indices are close to each other.

5.5. Examination of the m_c versus δ Relation

m_c versus δ curves for different r values are given below.

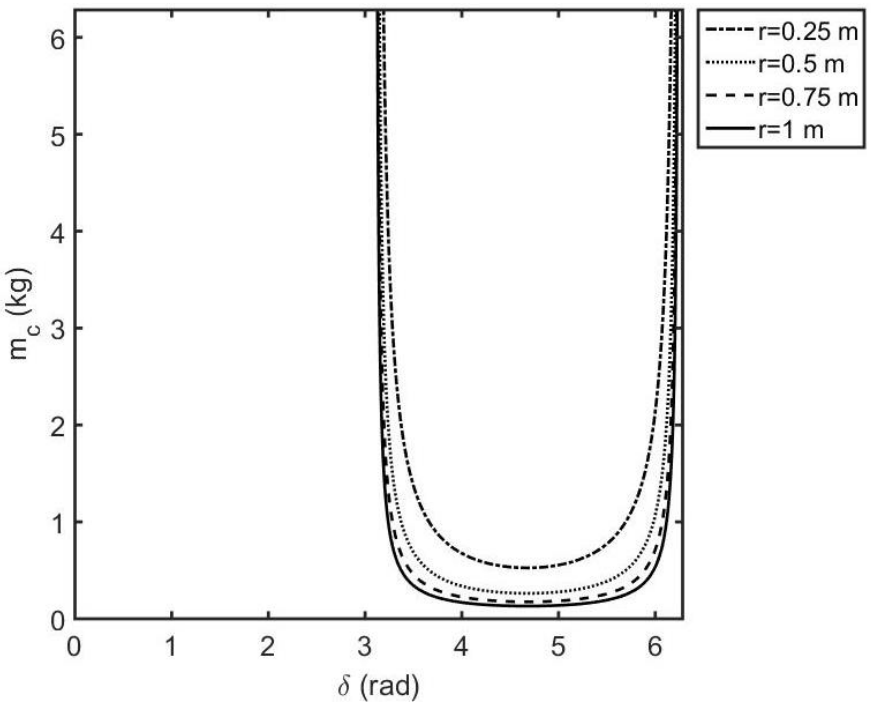

Figure 5.8 m_c vs. δ for different r values

Figure 5.8 shows a similar trend to that of Figure 5.6. Reason of this is that, $m_c r$ term is dominant compared to $m_c r^2$ term in the balance design equation (4.14).

Table 5.5 Performance indices for some points selected on Figure 5.8

Case	r (m)	m_c (kg)	$m_c r$ (kg.m)	δ (rad)	Performance Index
5.1	1	0.5027	0.5027	3.3715	303.1426
5.2		0.4000	0.4000	3.4417	245.8448
5.3		0.1324	0.1324	4.7972	62.6597
5.4		0.1545	0.1545	5.2314	50.1548
5.5		0.6809	0.6809	6.0542	308.1490
5.6	0.75	0.6701	0.5026	3.3715	302.0530
5.7		0.5334	0.4000	3.4417	244.9572
5.8		0.1765	0.1324	4.7972	62.5933
5.9		0.2061	0.1546	5.2314	50.0359
5.10		0.9079	0.6809	6.0542	308.8991
5.11	0.5	1.0052	0.5026	3.3715	301.5082
5.12		0.8001	0.4000	3.4417	244.5133
5.13		0.2648	0.1324	4.7972	62.7565
5.14		0.3091	0.1546	5.2314	50.1284
5.15		1.3619	0.6809	6.0542	309.5506
5.16	0.25	2.0105	0.5026	3.3715	302.5569
5.17		1.6002	0.4000	3.4417	245.4182
5.18		0.5296	0.1324	4.7972	62.5599
5.19		0.6182	0.1546	5.2314	49.9764
5.20		2.7237	0,6809	6.0542	309.6491

Examining Table 5.5 leads the following conclusions: For the cases with the same $m_c r$ value, the performance indices are nearly the same (see cases 5.1, 5.6, 5.11 and 5.16). Again the performance index increases as the $m_c r$ value increases. An exception to this is encountered when cases 5.3 and 5.4 are compared. Another observation is that when

$\delta \cong \pi$ or $\delta \cong 2\pi$, the performance index gains significantly high values (see cases 5.1, 5.2, 5.5). In between these values, the performance index takes significantly smaller values (see cases 5.3, 5.4).

5.6. Examination of the m_c versus I_c Relation

For completeness of the work, m_c versus I_c graph is also given in Figure 5.9.

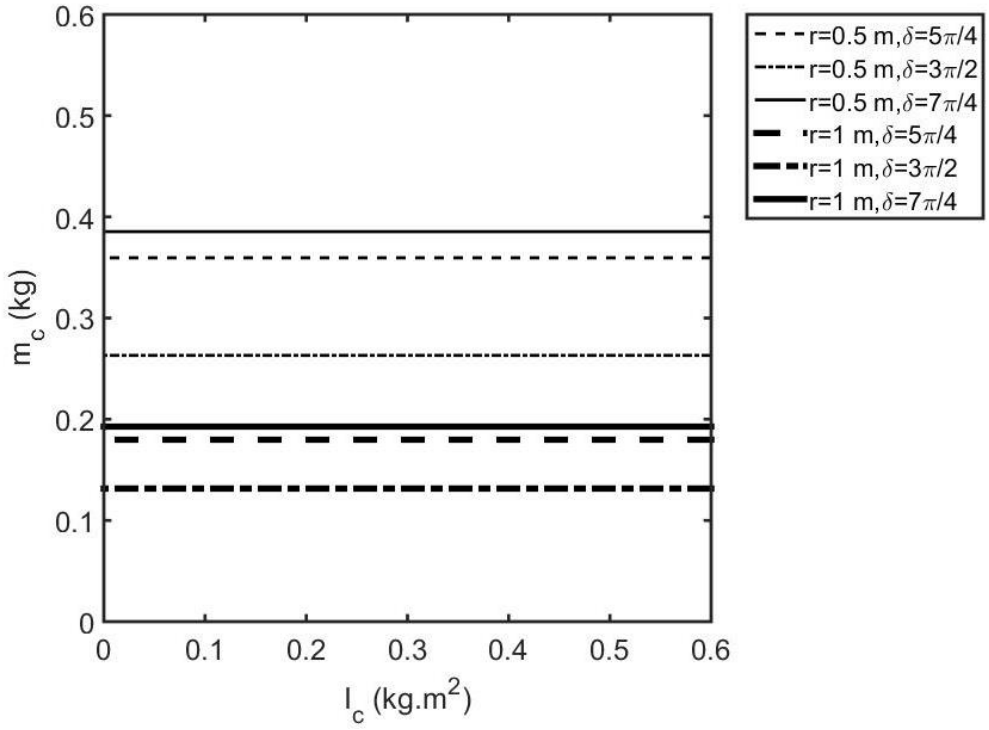

Figure 5.9 m_c vs. I_c for different r and δ pairs

As discussed previously, the value of I_c does not have a significant effect on the suitable m_c values for a given r and δ.

Table 5.6 Performance indices for some points selected on Figure 5.9

Case	$r\ (\mathrm{m})$	$\delta\ (\mathrm{rad})$	$m_c\,(\mathrm{kg})$	Performance Index
6.1	0.5	$\frac{5\pi}{4}$	0.359	109.1109
6.2		$\frac{6\pi}{4}$	0.263	64.7774
6.3		$\frac{7\pi}{4}$	0.385	67.2269
6.4	1	$\frac{5\pi}{4}$	0.180	109.4718
6.5		$\frac{6\pi}{4}$	0.132	64.8653
6.6		$\frac{7\pi}{4}$	0.193	67.1356

Table 5.6 also supports the previous conclusions. Examining cases 6.1 and 6.4 suggests that the performance index does not change dramatically for the same δ value and that the suitable $m_c r$ values are nearly the same for the same δ value.

6. CONCLUSION

There are numerous approaches for singularity crossing problem of parallel robots [9-16]. But only singularity robust balancing [18] and singularity consistent payload placement [19] methods enables to pass through inconsistent trajectories.

In this thesis, different scenarios are analyzed by applying singularity robust balancing method to 3-RPR manipulators. In this manner, first of all, kinematic and dynamic analyses of the mechanism are performed. Then three counterweights are introduced, and the balance design equation is obtained. With using this equation, suitable counterweight loci are determined. Two theorems and two corollaries are proposed within this context. Then, a numerical case study is conducted and different balancing scenarios are compared according to a performance index that takes into account the actuator forces.

For the considered numerical example, it is seen that the effect of the mass moments of inertia of the counterweights is negligible compared to those of the other balancing parameters. There are no solutions for some certain values of δ , and performance index does not change dramatically once δ is kept fixed. Moreover, when $\delta \cong \pi$ or $\delta \cong 2\pi$ performance index gains significantly high values. Almost at the middle of this interval, the performance index attains its lowest value. Also, in order to have a solution, δ should be within the interval $3.1069 < \delta < 6.2485$. Therefore, δ shall be considered as one of the main factors that affect the performance index.

Furthermore, in the balance design equation (4.14), the numerical value of the coefficient of the term including $m_c r^2$ is quite small. Because of this reason, the effect of this term is negligible and, instead of treating m_c and r variables separately they can be treated as a single parameter $m_c r$. Even though there are some exceptions, it is observed that as $m_c r$ increases, performance index increases. Hence, it can be said that the $m_c r$ parameter is another main factor that affects the performance index.

Finally, it can be seen that the performance index changes in a wide range depending on the selected counterweight parameters. Due to this reason, choice of the numerical values for the counterweight parameters is critical. It is worth to mention that the conclusions drawn above for the numerical case study will differ for different manipulator parameters and for a different trajectory. However, any case can be analyzed in the same manner by using the derived general balance design equation (3.48) and the proposed theorems here.

As a future work, counterweights, elastic elements and dampers can be applied together to further decrease the performance index while using the singularity robust balancing method on the 3-RPR mechanism.

REFERENCES

[1] Zhang, D., Su, X., Gao, Z., & Qian, J. (2013). Design, analysis and fabrication of a novel three degrees of freedom parallel robotic manipulator with decoupled motions. *International Journal of Mechanics and Materials in Design*, *9*(3), 199–212.

[2] Staicu, S. K. (2012). Matrix modeling of inverse dynamics of spatial and planar parallel robots. *Multibody System Dynamics*, *27*(2), 239–265.

[3] Boudreau, R., & Nokleby, S. (2012). Force optimization of kinematically-redundant planar parallel manipulators following a desired trajectory. *Mechanism and Machine Theory*, *56*, 138–155.

[4] Choi, H. B., & Ryu, J. (2012). Singularity analysis of a four degree-of-freedom parallel manipulator based on an expanded 6 x 6 Jacobian matrix. *Mechanism and Machine Theory*, *57*, 51–61.

[5] Gosselin, C., & Angeles, J. (1990). Singularity analysis of closed-loop kinematic chains. *IEEE Transactions on Robotics and Automation*, *6*(3), 281-290.

[6] Choudhury, P., & Ghosal, A. (2000). Singularity and controllability analysis of parallel manipulators and closed-loop mechanisms. *Mechanism and Machine Theory*, *35*(10), 1455–1479.

[7] Jui, C. K., & Sun, Q. (2005). Path tracking of parallel manipulators in the presence of force singularity. *Journal of Dynamic Systems, Measurement, and Control*, *127*(4), 550-563.

[8] Daniali, H. M., Zsombor-Murray, P. J., & Angeles, J. (1995). Singularity analysis of planar parallel manipulators. *Mechanism and Machine Theory*, *30*(5), 665-678.

[9] Bohigas, O., Henderson, M. E., Ros, L., Manubens, M., & Porta, J. M. (2013). Planning singularity-free paths on closed-chain manipulators. *IEEE Transactions on Robotics*, *29*(4), 888-898.

[10] Dasgupta, B., & Mruthyunjaya, T. S. (1998). Force redundancy in parallel manipulators: theoretical and practical issues. *Mechanism and Machine Theory*, *33*(6), 727-742.

[11] Ganovski, L., Fisette, P., & Samin, J. C. (2004). Piecewise overactuation of parallel mechanisms following singular trajectories: Modeling, simulation and control. *Multibody System Dynamics*, *12*(4), 317-343.

[12] Agarwal, A., Nasa, C., & Bandyopadhyay, S. (2016). Dynamic singularity avoidance for parallel manipulators using a task-priority based control scheme. *Mechanism and Machine Theory*, *96*, 107-126.

[13] Ider, S. K. (2004). Singularity robust inverse dynamics of planar 2-RPR parallel manipulators. *Proceedings of the Institution of Mechanical Engineers, Part C: Journal of Mechanical Engineering Science*, *218*(7), 721–730.

[14] Ider, S. K. (2005). Inverse dynamics of parallel manipulators in the presence of drive singularities. *Mechanism and Machine Theory*, *40*(1), 33–34.

[15] Briot, S., & Arakelian, V. (2008). Optimal force generation in parallel manipulators for passing through the singular positions. *The International Journal of Robotics Research*, *27*(8), 967-983.

[16] Briot, S., Pagis, G., Bouton, N., & Martinet, P. (2016). Degeneracy conditions of the dynamic model of parallel robots. *Multibody System Dynamics*, *37*(4), 371-412.

[17] Özdemir, M. (2017). Removal of singularities in the inverse dynamics of parallel robots. *Mechanism and Machine Theory*, *107*,71–86.

[18] Özdemir, M. (2016). Singularity robust balancing of parallel manipulators following inconsistent trajectories. *Robotica*, *34*(9), 2027-2038.

[19] Özdemir, M. (2016). Singularity-consistent payload locations for parallel manipulators. *Mechanism and Machine Theory*, *97*, 171-189.

[20] Özdemir, M. (2017). Dynamic analysis of planar parallel robots considering singularities and different payloads. *Robotics and Computer-Integrated Manufacturing*, *46*, 114-121.

[21] Karimi, A., Masouleh, M. T., & Cardou, P. (2016). Avoiding the singularities of 3-RPR parallel mechanisms via dimensional synthesis and self-reconfigurability. *Mechanism and Machine Theory*, *99*, 189-206.

[22] Li, S., Liu, Y., Cui, H., Niu, Y., & Zhao, Y. (2016). Synthesis of branched chains with actuation redundancy for eliminating interior singularities

of 3T1R parallel mechanisms. *Chinese Journal of Mechanical Engineering*, *29*(2), 250-259.

[23] Liu, S., Qiu, Z. C., & Zhang, X. M. (2017). Singularity and path-planning with the working mode conversion of a 3-DOF 3-RRR planar parallel manipulator. *Mechanism and Machine Theory*, *107*, 166-182.

[24] Kaloorazi, M. H. F., Masouleh, M. T., & Caro, S. (2016). Determining the maximal singularity-free circle or sphere of parallel mechanisms using interval analysis. *Robotica*, *34*(01), 135-149.

[25] Liu, Y., Wu, J., Wang, L., & Wang, J. (2016). Determination of the maximal singularity-free zone of 4-RRR redundant parallel manipulators and its application on investigating length ratios of links. *Robotica*, *34*(09), 2039-2055.

[26] Özdemir, M., & Ider, S. K. (2016). A switching inverse dynamics controller for parallel manipulators around drive singular configurations. *Turkish Journal of Electrical Engineering & Computer Sciences*, *24*(5), 4267-4283.

[27] Dehkordi, M. B., Frisoli, A., Sotgiu, E., & Bergamasco, M. (2012). Modelling and experimental evaluation of a static balancing technique for a new horizontally-mounted 3-UPU parallel mechanism. *International Journal of Advanced Robotic Systems*, *9*(193).

[28] Perreault, S., Cardou, P., & Gosselin, C. (2014). Approximate static balancing of a planar parallel cable-driven mechanism based on four-bar linkages and springs. *Mechanism and Machine Theory*, *79*, 64–79.

[29] Russo, A., Sinatra, R., & Xi, F. (2005). Static balancing of parallel robots. *Mechanism and Machine Theory*, *40*(2), 191–202.

[30] Simionescu, I., Ciupitu, L., & Ionita, L. C. (2015). Static balancing with elastic systems of DELTA parallel robots. *Mechanism and Machine Theory*, *87*, 150–162.

[31] Jean, M., & Gosselin, C. M. (1996). Static balancing of planar parallel manipulators. *IEEE International Conference on Robotics and Automation*, *4*(April), 3732–3737 vol.4.

[32] Gosselin, C. M., & Wang, J. (2000). Static balancing of spatial six-degree-of-freedom parallel mechanisms with revolute actuators. *Journal of Robotic Systems*, *17*(3), 159–170.

[33] Laliberte, T., Gosselin, C. M., & Jean, M. (1999). Static balancing of 3-DOF planar parallel mechanisms. *IEEE/ASME Transactions on Mechatronics*, *4*(4), 363–377.

[34] Wang, J., & Gosselin, C. M. (2000). Static balancing of spatial four-degree-of-freedom parallel mechanisms. *Mechanism and Machine Theory*, *35*(4), 563–592.

[35] Wang, J., & Gosselin, C. M. (1999). Static balancing of spatial three-degree-of-freedom parallel mechanisms. *Mechanism and Machine Theory*, *34*(3), 437–452.

[36] Liu, T., Gao, F., Zhao, X., & Qi, C. (2014). Static balancing of a spatial six-degree-of-freedom decoupling parallel mechanism. *Journal of Mechanical Science and Technology*, *28*(1), 191–199.

[37] Wijk, V. Van Der, Demeulenaere, B., & Herder, J. L. (2009). Comparison of various dynamic balancing principles regarding additional mass and additional inertia. *ASME Journal of Mechanisms and Robotics*, *1*(4), 41006.

[38] Wijk, V. Van Der, & Herder, J. L. (2008). Double pendulum balanced by counter-rotary counter-masses as useful element for synthesis of dynamically balanced mechanisms. *ASME 2008 International Design Engineering Technical Conferences and Computers and Information in Engineering Conference*, 453–463.

[39] Arakelian, V. H., & Smith, M. R. (2008). Design of planar 3-DOF 3-RRR reactionless parallel manipulators. *Mechatronics*, *18*(10), 601–606.

[40] Wang, K., Li, K., Zhang, Q., Luo, M., & Chen, P. (2016). Enhanced active dynamic balancing of the planar robots using a three-rotating-bar balancer. *Advances in Mechanical Engineering*, *8*(4), 1687814016643885.

[41] Gosselin, C. M., Vollmer, F., Côté, G., & Wu, Y. (2004). Synthesis and design of reactionless three-degree-of-freedom parallel mechanisms. *IEEE Transactions on Robotics and Automation*, *20*(2), 191–199.

[42] Wu, Y., & Gosselin, C. M. (2004). Synthesis of reactionless spatial 3 - DOF and 6 - DOF mechanisms without separate counter - rotations. *The International Journal of Robotics Research*, *23*(625–642).

[43] Laliberté, T., & Gosselin, C. (2016). Synthesis, optimization and experimental validation of reactionless two-DOF parallel mechanisms using counter-mechanisms. *Meccanica*, *51*(12), 3211-3225.

[44] Arakelian, V., & Briot, S. (2008). Dynamic balancing of the SCARA robot. *Proceedings of 17th CISM-IFToMM (Center International Des Sciences Mechaniques and International Federation for the Promotion of Mechanism and Machine Science) Conference on Robot Design, Dynamics and Control*.

[45] Briot, S., & Arakelian, V. (2009). Complete shaking force and shaking moment balancing of the position-orientation decoupled PAMINSA manipulator. *IEEE/ASME International Conference on Advanced Intelligent Mechatronics, AIM*, 1521–1526.

[46] Wijk, V. Van Der, Herder, J. L., Demeulenaere, B., & Gosselin, C. (2012). Comparative analysis for low-mass and low-inertia dynamic balancing of mechanisms. *ASME Journal of Mechanisms and Robotics*, *4*(3), 0311008.

[47] Wijk, V. Van Der, & Herder, J. L. (2008). Dynamic balancing of mechanisms by using an actively driven counter-rotary counter-mass for low mass and low inertia. *Proceedings of the Second International Workshop on Fundamental Issues and Future Research Directions for Parallel Mechanisms and Manipulators*, 241–251.

[48] Wijk, V., & Herder, J. L. (2009). Guidelines for low mass and low inertia dynamic balancing of mechanisms and robotics. *Advances in Robotics Research*, 21-30.

[49] Van Der Wijk, V. (2017). Design and analysis of closed-chain principal vector linkages for dynamic balance with a new method for mass equivalent modeling. *Mechanism and Machine Theory*, *107*, 283-304.

[50] Arakelian, V. (2014). Shaking force and shaking moment balancing in robotics: a critical review. In *Advances on Theory and Practice of Robots and Manipulators* (pp. 149-157). Springer International Publishing.

[51] Gosselin, C. (2008). Gravity compensation, static balancing and dynamic balancing of parallel mechanisms. *Smart Devices and Machines for Advanced Manufacturing*, 27–48.

[52] Kong, X., & Gosselin, C. M. (2001). Forward displacement analysis of third-class analytic 3-RPR planar parallel manipulators. *Mechanism and Machine Theory*, *36*(9), 1009–1018.

[53] Staicu, S. (2009). Power requirement comparison in the 3-RPR planar parallel robot dynamics. *Mechanism and Machine Theory*, *44*(5), 1045–1057.

[54] Zein, M., Wenger, P., & Chablat, D. (2008). Non-singular assembly-mode changing motions for 3-RPR parallel manipulators. *Mechanism and Machine Theory*, *43*(4), 480–490.

[55] Wenger, P., Chablat, D., & Zein, M. (2007). Degeneracy study of the forward kinematics of planar 3-RPR parallel manipulators. *Journal of Mechanical Design*, *129*(12), 1265–1268.

[56] Arakelian, V. H., & Smith, M. R. (2008). Design of planar 3-DOF 3-RRR reactionless parallel manipulators. *Mechatronics*, *18*(10), 601–606.

[57] Yong, Y. K., & Lu, T. F. (2009). Kinetostatic modeling of 3-RRR compliant micro-motion stages with flexure hinges. *Mechanism and Machine Theory*, *44*(6), 1156–1175.

[58] Wu, J., Wang, J., Wang, L., & You, Z. (2010). Performance comparison of three planar 3-DOF parallel manipulators with 4-RRR, 3-RRR and 2-RRR structures. *Mechatronics*, *20*(4), 510–517.

[59] Kucuk, S. (2013). Energy minimization for 3-RRR fully planar parallel manipulator using particle swarm optimization. *Mechanism and Machine Theory*, *62*, 129–149.

[60] Zhang, X., Mills, J. K., & Cleghorn, W. L. (2007). Dynamic modeling and experimental validation of a 3-PRR parallel manipulator with flexible intermediate links. *Journal of Intelligent and Robotic Systems: Theory and Applications*, *50*(4), 323–340.

[61] Zhang, X., Wang, X., Mills, J. K., & Cleghorn, W. L. (2008). Dynamic modeling and active vibration control of a 3-PRR flexible parallel manipulator with PZT transducers. *Proceedings of the World Congress on Intelligent Control and Automation (WCICA)*, *26*(2008), 461–466.

[62] Zhang, X., Mills, J. K., & Cleghorn, W. L. (2009). Coupling characteristics of rigid body motion and elastic deformation of a 3-PRR parallel manipulator with flexible links. *Multibody System Dynamics*, *21*(2), 167–192.

[63] Staicu, S. (2009). Inverse dynamics of the 3-PRR planar parallel robot. *Robotics and Autonomous Systems*, *57*(5), 556–563.

[64] Karimi, A., Masouleh, M. T., & Cardou, P. (2016). Avoiding the singularities of 3-RPR parallel mechanisms via dimensional synthesis and self-reconfigurability. *Mechanism and Machine Theory*, *99*, 189–206.

[65] Moezi, S. A., Rafeeyan, M., Zakeri, E., & Zare, A. (2016). Simulation and experimental control of a 3-RPR parallel robot using optimal fuzzy controller and fast on/off solenoid valves based on the PWM wave. *ISA Transactions*, *61*, 265–286.

[66] Farajtabar, M., Daniali, H. M., & Varedi, S. M. (2015). Pick and place trajectory planning of planar 3-RRR parallel manipulator in the presence of joint clearance. *Robotica*, *35*(March), 1–13.

[67] Varedi-Koulaei, S. M., Daniali, H. M., Farajtabar, M., Fathi, B., & Shafiee-Ashtiani, M. (2016). Reducing the undesirable effects of joints clearance on the behavior of the planar 3-RRR parallel manipulators. *Nonlinear Dynamics*, *86*(2), 1007–1022.

[68] Zhang, Q., Mills, J. K., Cleghorn, W. L., Jin, J., & Zhao, C. (2015). Trajectory tracking and vibration suppression of a 3-PRR parallel manipulator with flexible links. *Multibody System Dynamics*, *33*(1), 27–60.

CURRICULUM VITAE

PERSONAL INFORMATION

Surname, Name: Süülker,Cem

Nationality: Turkish (T.C.)

Date and Place of Birth: 22.09.1993, İstanbul

E-mail: suulkercem@gmail.com

EDUCATION

Degree	Institution	Date of Graduation	C.GPA
B.S.	Marmara University Department of Mechanical Engineering, İstanbul	14.06.2016	2.79/4

WORK EXPERIENCE

Period	Place	Position
September 2013 - June 2016	Marmara University Department of Mechanical Engineering, İstanbul	Student Assistant
April 2018 - Present	İstanbul Okan University Department of Mechanical Engineering, İstanbul	Research Assistant

PUBLICATIONS FROM THE THESIS

1. **Özdemir, M., Süülker, C.**, (2018). Counterweight Balancing of a 3-RPR Planar Parallel Robot for Passing through a Singularity. *9th International Automotive Technologies Congress (OTEKON 2018), 7-8 May 2018, Bursa*, Turkey, pp. 1060-1067.